Influence of Equilibrium Initialisation on Human Body Model Responses in Crash Simulations

Hanna Mirkhan, Jobin D. John, Johan Iraeus

Abstract Although finite element human body models (HBM) enable more biofidelic virtual testing for injury assessment, compared to anthropomorphic test devices, workflows for consistent evaluations are not yet formalised. Most current workflows rely on gravity settling before a crash simulation, yet the specifics of the settling procedure vary in the literature. This study quantifies how the initialization of an HBM influences its crash kinematics and kinetics by comparing three approaches categorised by the state of HBM-seat equilibrium at the start of the crash loading – (1) full quasi-static equilibrium, (2) partial equilibrium through solver-initialised stresses in the seat foam and HBM hip, and (3) no equilibrium. Six models from three lineups (VIVA+ 50F and 50M, THUMS 05F, 50M, and 95M, and SAFER HBM 50M) that represent diverse anthropometries and modelling approaches, were simulated in frontal and rear impacts, to generalise the results.

Across all HBMs, lack of full equilibrium led to systematic downward movement of the head by up to 20 mm accompanied with higher vertical seat forces while compressing the spine. Although this downward movement is also seen during the gravity settling in the full equilibrium case, for the partial and non-equilibrium it occurred in the crash phase. Peak forward (in frontal) and backwards (in rear) displacements were less affected, generally differing by less than 10 mm between the full equilibrium and the other two versions.

Due to the compliant soft tissues and deformable spinal structures in HBMs, conventional crash test dummy-based initialisation does not lead to equilibrium for HBM simulations. This incomplete equilibrium can alter the kinematics during the crash, influencing the HBM's interaction with the restraint system. This study highlights the importance of defining consistent initialisation procedures that ensure comparable evaluations in virtual testing.

Keywords Gravity settling, Human body model, Initial Equilibrium, Stress-initialisation, Virtual Testing.

I. INTRODUCTION

Virtual testing as a complement to physical testing for injury assessment in vehicle crashes has been evolving swiftly in recent years, with broad efforts to establish protocols and workflows [1–7]. In these virtual tests, the virtual human body representations are either finite element (FE) models of anthropometric test devices (ATDs), also called crash test dummies, or FE models of the detailed anatomical human body itself, normally called Human Body Models (HBMs). ATDs and their virtual equivalents are limited in their biofidelity due to simplified skeletal structures, limited anatomical segmentation, and idealised mechanical representations. By contrast, HBMs hold the promise of a more biofidelic injury assessment due to the possibility of accurate representation of anatomical geometry and material properties [8].

However, the advantages that make HBMs more biofidelic also introduce new challenges in crash simulations, mainly related to the initialisation of simulations. Initialising an HBM to represent a seated human in a vehicle interior normally involves deforming it from the default posture [9] and positioning it in a deformable seat. The method to position ATDs is well defined and involves using the seat H-point (defined using the H-point manikin) as base line, followed by repositioning the limbs using well defined mechanical joints. The "H-point" of HBMs (and real humans) are however less well defined as it will vary not only by seat parameters, but also by the soft tissue shape/properties around the hip. In addition, HBMs (and real humans) have joints where the joint axis changes over the joint rotation. At present, positioning an HBM to a target posture is normally achieved using either the marionette method or through mesh morphing [10].

More specifically, HBMs do not interact with the vehicle seat in the same way as ATDs during model

H. Mirkhan is a MSc student in Applied Mechanics, J.D. John (jobin.john@chalmers.se, +46317726597) and J. Iraeus are Researchers at the Vehicle Safety Division at the Department of Mechanical Engineering at Chalmers University of Technology, Sweden.

initialisation, as the soft tissues in HBMs are much softer than the soft tissues of ATDs. While the soft tissue of ATDs principally stay undeformed when the ATD is seated in a vehicle seat and loaded purely by gravity, the soft tissue stiffness of HBMs (and real humans) are comparable to the seat foam, and thus both the soft tissue and the seat foam will deform when loaded under gravity.

Methods to initialise a crash simulation using ATDs mainly focus on deforming the seat foam, with or without retaining the initial stress state from that deformation [11]. There are efficient methods to do this in pre-processors, and after starting the simulation with or without dynamic relaxation, the crash pulse can be applied directly. At time zero, the seat foam will try to spring back to the undeformed state, pushing on the ATD soft tissues. Consequently, as these soft tissues are stiff compared to the seat foam, and as the ATD spine is rather rigid, all the ATD upper body mass will reach equilibrium with the seat forces under the influence of gravity rather promptly.

HBMs on the other hand have more compliant soft tissues and a deformable spine, meaning that using the standard ATD initialisation method won't ensure equilibrium shortly after the simulation starts. Instead, the "gold standard" approach to initialise HBMs in equilibrium is therefore to start the simulation with a period when only gravity is added, allowing the HBM to settle into the seat, before applying the crash pulse. The length of this period varies greatly in reported studies, from 150 milliseconds to 800 milliseconds [9,12–15]. Oscillations in contact force and HBM position are typically seen during this step, for example see [9], and these are gradually damped by the material damping in the seat foam and HBM soft tissues.

To the best of the authors' knowledge there is only one study in which gravity settling of HBMs has been studied in a systematic way [16]. In that study, the authors pursued an optimal settling time, estimated through several parameters measuring closeness to equilibrium. 350ms was suggested for upright occupants and 290ms for reclined occupants. Despite a large number of simulations, the effect the equilibrium (or lack thereof), had on the crash response was only evaluated in five simulations. In addition, only one HBM and only one seat model was used. As such, a fundamental question remains unanswered: How much effect does the (lack of) equilibrium in HBM initialisation have on the crash response? The aim of this study is therefore to quantify the influence of HBM to seat equilibrium attained due to initialisation choices on the HBM crash response.

II. METHODS

To evaluate the influence of HBM initialisation on the kinetics and kinematics in the crash phase, three initialisation approaches were compared in this study. The three approaches represent different equilibrium states (achieved not only between the HBM and seat, but also within the HBM) at beginning of the crash pulse. In descending order of closeness to the true equilibrium, these will be referred to as: Full equilibrium (FEq), Partial equilibrium (PEq), and No-equilibrium (NEq). The crash pulse in the FEq simulations was delayed until quasi-static equilibrium under gravity was achieved. For the NEq and PEq simulations the seat foam and HBM soft tissue were already pre-deformed at the start of the simulation, and the crash pulse was applied directly at time zero. While the PEq simulations had a solver-enforced equilibrium at the start of the crash pulse, which involved initialising the stress state in the simulation based on a reference geometry of the HBM and seat, no stress initialisation was included for the NEq simulations.

All three equilibrium approaches were simulated for six HBM models (VIVA+ 50F & 50M v1.0.1, THUMS 05F, 50M, 95M v4.1, and SAFER HBM 50M v2.0.0), representing variability both in anthropometrics (5th female to 95th Male) and HBM implementation (VIVA+, THUMS, and SAFER HBM). All HBMs were implemented in their original posture, i.e. no preprocessing step was used to align spine curvature, the leg or arm angles. For the crash phase, two load cases, one frontal crash and one rear crash, were studied.

Full Equilibrium (FEq) Initialisations

As the first step in establishing the FEq simulation, each HBM was positioned just above the seat and allowed to fall under gravity loading during a 1000ms transient simulation, long enough to capture several oscillations when the HBM bounces up and down on the seat, see for example Fig. A1 in the Appendix. To find the target position, first the fore-aft and vertical position of the different sized HBMs was adjusted so the right foot was just touching the gas pedal with the heel just above the floor. Here, only translations, i.e. no rotation was applied to position the HBMs. Next, the seat was adjusted horizontally and vertically to match the different HBM target positions. Horizontally it was adjusted so the HBM back had about 10 mm intersection with the backrest, and vertically until the hip intersected the seat base with approximately 20mm. Finally, the HBM was translated upwards until the hip and back just cleared the seat surface*, before starting the gravity settling simulation*. The head and spine (at each vertebrae level) were constrained in longitudinal (anterior-posterior) and lateral (medial-lateral) directions to help the HBM keep the posture during settling. Additionally, the hands were constrained in all DOF's, applied after a specified time (to allow the hands to settle down together with the body). This specified time was 115ms for the THUMS models, 150ms for the SAFER HBM and 110ms for the VIVA+ models. At the start of the crash phase all these constraints were terminated, allowing the spine, head and hands to move freely. As mentioned above, the different HBMS were implemented in their original posture. As the head and spine was constrained during the gravity settling, the HBMs retained the spine curvature. The extremities joint angles did however change slightly during the settling, as the thighs interacted with the seat base, and the hands were locked to the steering wheel after some initial settling. These changes were however small.

In order to reach quasi-static equilibrium as fast as possible, global damping was added next. Following the LS-DYNA user's manual, the undamped response should be used to determine ω, the lowest (fundamental) eigenfrequency corresponding to the longest eigenperiod of the system [17]. The manual recommends using a damping factor of 2ω to achieve critical damping. However, as the baseline model including the seat foam and HBM soft tissues already are damped on material level, the system is not undamped and hence applying 2ω (based on the measured eigenperiod) resulted in overdamped responses for all HBMs. Iteratively reducing the damping factor showed that using ω, instead of 2ω, yielded responses close to critically damping. The setup was considered to be in equilibrium when the absolute velocity of a point at the anterior superior iliac spine (ASIS) was, and stayed, below 0.005 m/s. The time to equilibrium was noted, and a third simulation was run where the global damping was ramped down to zero over a period of 50ms, starting from the recorded equilibrium time. Finally, the crash pulse was delayed, starting after the damping was ramped down, meaning that the total simulation time for the FEq simulations were *time to equilibrium + 50 ms* damping ramp down + *150 ms for the crash pulse*.

Partial Equilibrium (PEq) and No-Equilibrium (NEq) Initialisations

The starting point used in the PEq and NEq simulations was the deformed geometries of the HBM and the seat from the FEq simulation, after the ramping down of the damping. These geometries were obtained by outputting the nodal coordinates and using these as input to the NEq and PEq simulations. For both versions, the crash pulse and gravity loading was applied directly at the start of the simulation. For the PEq simulation the undeformed geometry of the seat foam and the HBM soft tissues around the pelvis and thighs were included in the "reference geometry" to initialise stresses in the material of these parts, while for the NEq no stresses were initialised.

Crash Simulations

All the simulations were run with LS-DYNA v12.2.1 on the same HPC cluster using either 32 or 64 cores (across all equilibrium comparisons), to minimise the effect of numerical noise due to the solver decomposition of the model [18]. All results are reported using the SAE J211 convention, where the local x-direction is posterior-anterior, and the local z-direction is superior-inferior (or proximal-distal at extremities) [19]. The forces are reported as the environment acting on the HBM in the coordinate system according to SAE J1733, with x-direction pointing towards the vehicle front, and z-direction pointing downward [20].

For all three initialisations (FEq, PEq, and NEq) and all six HBMs, one frontal- and one rear end crash pulse were tested and analysed (Fig. 1). As a surrogate for a vehicle environment, a generic model of the vehicle interior was used [21]. In this model the occupant is restrained by a standard pretensioned three-point seat belt with load limiter 4kN and a 350 mm radii driver airbag (DAB), both triggering at 10ms (in the frontal load case). As special focus of the current study is on the HBM settling, the original generic seat model in the vehicle interior model was replaced with a validated FE model of a 2010-2012 Toyota Auris front seat [22]. The setup can be seen in Fig. 1. The same parameter settings were used for all HBMs. The seat was adjusted in x-and z direction for the different sized HBMs to reach the pedals and the steering wheel. However, the height of the head rest was not adjusted. The frontal crash was simulated using a generic crash pulse, with a delta-V of 70 kilometers per hour, and the pulse shape parameter EV1 set to 3 making this a rather tough pulse [21]. In addition, 100 mm of instrument panel and 200 mm floor pan deformation were added, effectively pushing the steering wheel inboards. The rear crash used a mid-Euro NCAP crash pulse [23]. Both the frontal and rear crash were simulated for a duration of 150 ms. Just prior to applying the crash pulse, the constraints used to hold the head, spine and hands during the settling, were terminated.

Influence of Settling Approaches on HBM Responses

The influence of the three equilibrium initialisations on the HBM responses was primarily evaluated by comparing the nodal displacements at the head (centre of gravity), T1 vertebral body, T8 vertebral body, and pelvis (ASIS point). The FEq was considered the ground truth, with the PEq and NEq being compared to this. Additionally, the interaction of the HBM with the vehicle interior was compared using the contact forces between each HBM and its environment. In the frontal crash, this included the contact forces of seat belt, seat base, and driver airbag, while in the rear crash it included the seat and head restraint.

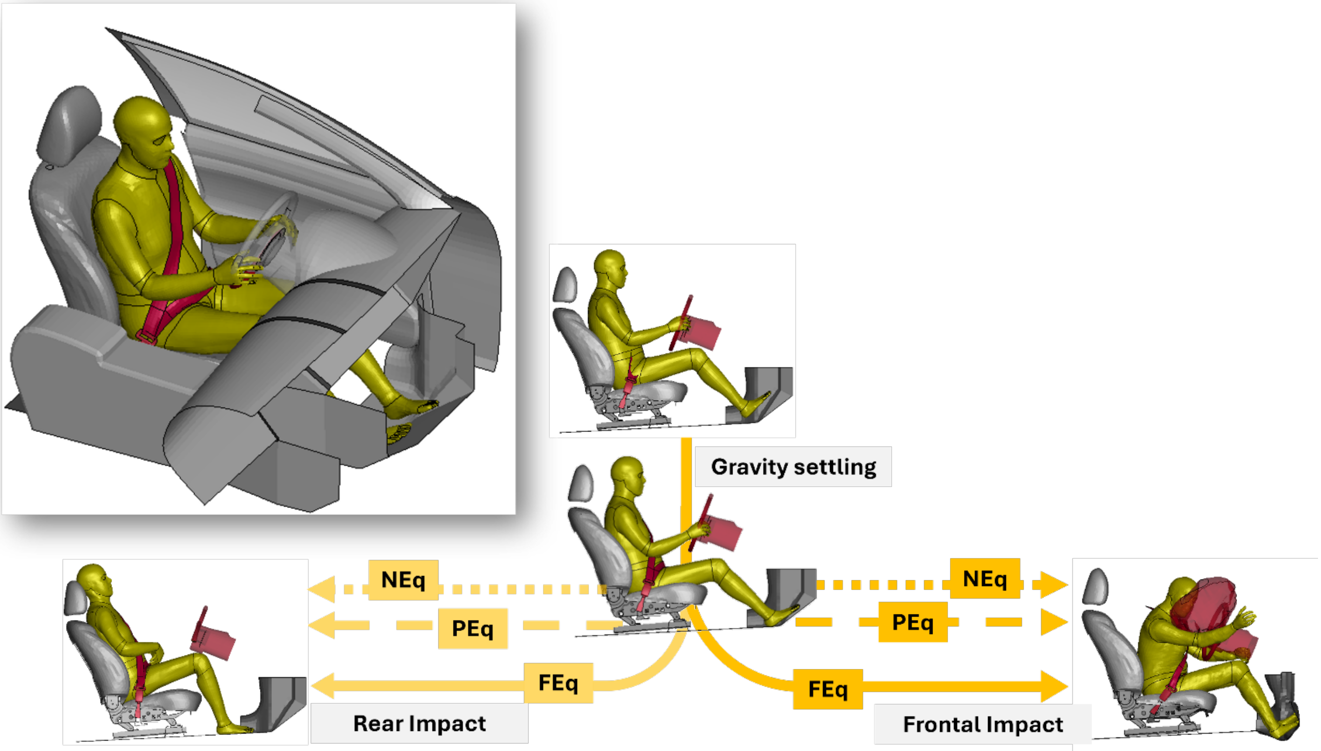

Fig. 1: Overview of the frontal and rear impact simulations, illustrated using the VIVA+ 50M model. The sequence shows pre-simulation position, gravity-settled position, and the position after 150 ms of crash simulation. In the Full Equilibrium (FEq) simulations, gravity was first applied along with a near-critical damping, after which the crash pulse was applied – all in a single simulation (represented by the continuous solid lines). The Partial Equilibrium (PEq) and No-Equilibrium (NEq) simulations used the geometry obtained at the end of FEq gravity-settling phase as the starting point of the simulation (represented by the dashed and dotted lines originating from the gravity settled geometry). PEq simulations have the stresses initialised in the seat and soft tissues around the pelvis and thighs. The line style as shown here for FEq (solid line), PEq (dashed line), and NEq (dotted line) is used in the rest of the figures to show their responses.

III. RESULTS

All 36 crash simulations (three Equilibrium conditions × six HBMs × two load cases) terminated without errors. The natural eigenfrequency (ω) varied over the six HBMs settling into the seat, with critical damping factors ranging from 0.196 to 0.276 ms^{-1}. The undamped and damped responses for the six HBMs are shown in Figures A1, B1, C1, D1, E1, F1 in the Appendix. The time to reach quasi-static equilibrium ranged from 360 to 760 ms for the different HBMs.

Frontal Crash Simulations

The x- and z-trajectories of the head, T1, T8, and ASIS nodes in the frontal crash simulations, for all HBMs, and all three equilibrium conditions, are shown in Fig. 2. All HBMs show similar relative patterns, where the head and thoracic spine landmarks of the PEq and NEq gradually drop down (in the z-direction), compared to the FEq, as the body moves forward (in positive x). For most of the traces, the difference between the PEq and NEq is small compared to the difference to the FEq, i.e. the PEq and NEq traces are close to each other, but away from the FEq. This drop down in z, is in most HBMs associated with less peak forward displacement. The difference is smaller for the ASIS landmark, and here the PEq trace is noticeably closer to the FEq trace for some of the HBMs, compared to the NEq trace.

A comparison of the peak (over time) x-displacement in each of the HBMs, and the peak z-displacement at the same time instance as peak x-displacement, is shown in Table I. For most landmarks, and most HBMs, the relative difference in peak x-displacement is less than 10 mm between the NEq or PEq and the FEq. However, in relative z-displacement it can be seen that for all HBMs, at least one of the measured nodes (Head, T1, or T8) drops down 10 mm or more in the NEq version. The addition of stress initiation in the PEq versions reduced the z drop down slightly, more for some models and less for others.

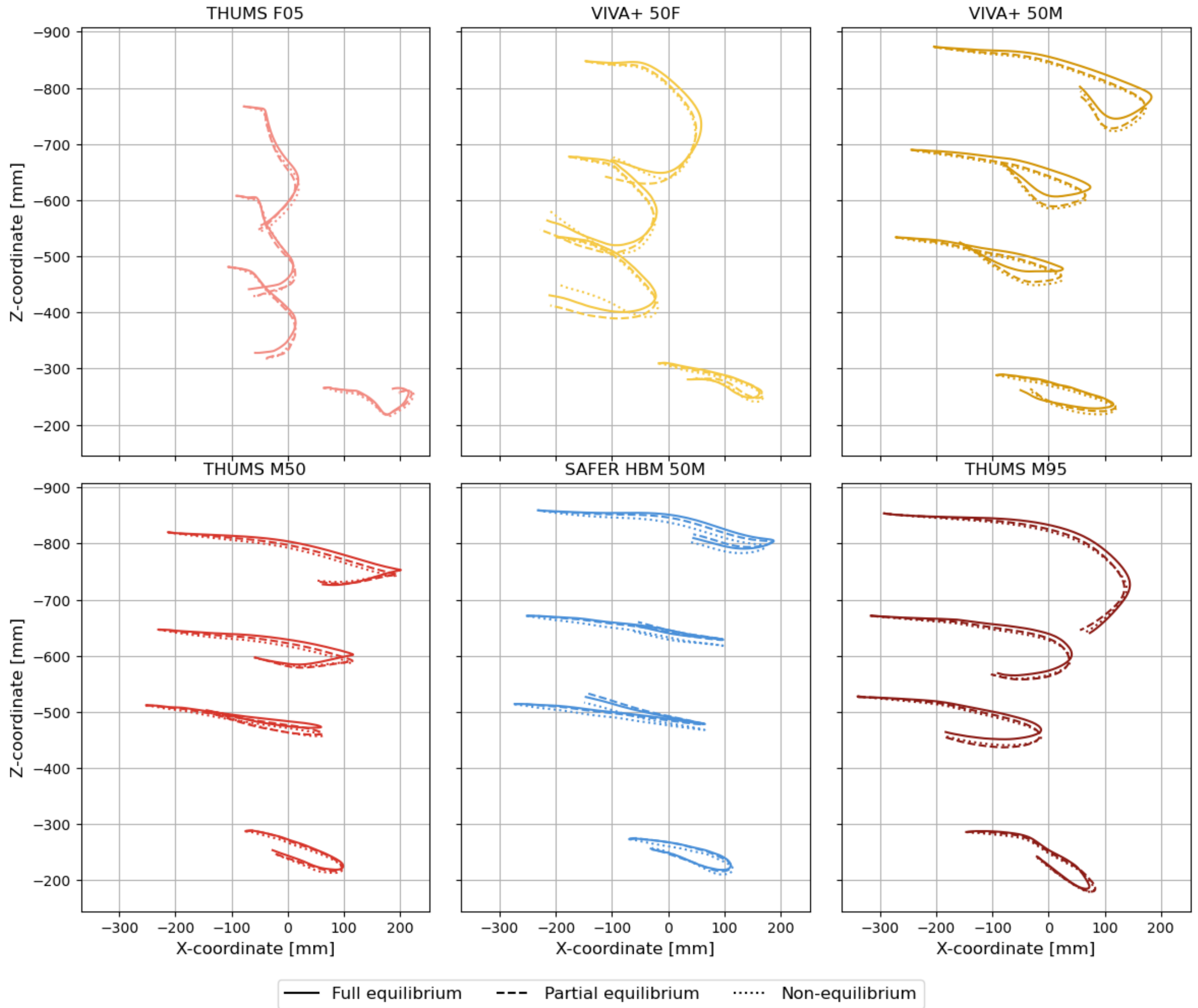

Fig. 2: Trajectories of the head, T1, T8 and pelvis in the front crash simulation, comparing the full equilibrium, to the partial and no equilibrium versions, for all six HBMs.

TABLE I
Differences in peak displacement in frontal crash (mm)
Difference between PEq or NEq and FEq.
Font format: 0-10 mm (light gray), 10-15 mm (normal), **15+ mm (bold)**

		Head (x)	T1 (x)	T8 (x)	ASIS (x)	Head (z)	T1 (z)	T8 (z)	ASIS (z)
THUMS 05F	*PEq*	-5.3	3.8	-0.4	9.1	12.1	14.9	**16.1**	1.2
	NEq	0.8	1.23	-0.0	12.2	13.1	6.1	10.3	2.7
VIVA+ 50F	*PEq*	-9.1	-5.7	-0.8	9.0	8.5	5.9	9.7	3.3
	NEq	-10.5	-2.8	3.5	9.3	**15.6**	**16.2**	**20.3**	7.5
VIVA+ 50M	*PEq*	-12.7	-8.9	-3.1	4.3	13.0	14.0	11.8	2.3

	NEq	-10.2	-7.3	-1.4	4.7	**19.2**	**18.1**	**17.5**	7.5
THUMS 50M	PEq	-7.5	-1.1	2.6	0.7	7.8	11.1	11.6	2.8
	NEq	-9.1	-3.2	2.9	1.6	10.3	14.3	**15.0**	5.5
SAFER HBM 50M	PEq	-4.4	0.8	-1.1	3.9	1.7	1.0	0.4	1.4
	NEq	-12.7	0.2	-0.5	7.0	8.6	11.3	10.4	7.0
THUMS 95M	PEq	-9.8	-4.7	-2.2	14.0	7.9	9.9	10.0	4.0
	NEq	-5.7	-2.1	0.6	12.0	9.3	8.6	11.5	4.4

The contact forces for the frontal crashes are shown in the Appendix as follows: Figures A2, B2, C2, D2, E2, and F2 show contact force over time for all three equilibrium conditions between HBM and seat base (x- and z-direction), HBM and DAB (x-direction), and HBM and belt; Figures A3, B3, C3, D3, E3, and F3 show peak contact force (independent of sign) for all three equilibrium conditions in all mentioned contacts. The differences in peak contact force are summarised in Table II. For all HBMs except the THUMS F05 model's contact force in the z-direction, the seat contact forces from the NEq differ more than those from the PEq. No clear pattern between the impact of using different methods and force direction was observed. Further, while the differences in the rest of the contacts, namely HBM to DAB and HBM to Belt, approach 500N at instances, the magnitude varies between contacts and equilibrium conditions.

TABLE II
Differences in peak contact force in frontal crash (N)
Difference between PEq or NEq and FEq.
Font format: 0-250 N (light gray), 250-500 N (normal), **500+ N (bold)**

		Seat base (x)	Seat base (z)	DAB (x)	Belt (x)
THUMS 05F	PEq	-112	-62	19	311
	NEq	-198	-35	-74	1
VIVA+ 50F	PEq	-41	-209	30	77
	NEq	-142	-453	24	-58
VIVA+ 50M	PEq	6	-30	374	-116
	NEq	9	107	262	-486
THUMS 50M	PEq	-41	-372	19	161
	NEq	-214	-475	-89	124
SAFER HBM 50M	PEq	0	-34	485	-125
	NEq	-163	274	488	-433
THUMS 95M	PEq	-59	431	59	-446
	NEq	-220	**533**	-37	-396

Rear End Crash Simulations

The x- and z-trajectories of the head, T1, T8, and ASIS nodes in the rear end impact, for all HBMs, and all three equilibrium conditions, are shown in Fig. 3. Also here, all HBMs show a similar relative pattern, where the head and thoracic spine landmarks of the PEq and NEq gradually drops down (in z-direction) compared to the FEq, as the body moves rearward (in negative x). For most of the traces, the difference between the PEq and NEq is small compared to the difference to the FEq, but for the rear end impact the effect of the stress initiation is larger than it was for the frontal crashes, meaning that the PEq is relatively closer to the FEq traces. This dropdown in z, is in most HBMs associated with less peak rearward displacement. Similar as for the frontal crash, the difference is smaller for the pelvis landmark, and also here the PEq is noticeably closer the FEq for most of the HBMs, compared to the NEq.

A comparison of the peak (in time) x-displacement in each of the case, and the peak z-diplacement at the same time instance as peak x-displacement is shown in Table III. For all landmarks and all HBMs, except the head CoG for THUMS M95 (which is the heaviest HBM that deforms the seat back most) the relative difference in x displacement is less than 10 mm, and even less than 5mm in most cases, comparing the NEq or PEq to the FEq. As for the frontal load case, it can be seen that in relative z-displacement, all HBMs drops down over 10 mm, and most over 15mm, for the Head, T1 and the T8 landmarks in the NEq version. In contrast to the frontal load case we can here see a more consistant effect of stress initiation in the PEq versions, where the z drop down is reduced to half or less for most of the models, compared to the NEq.

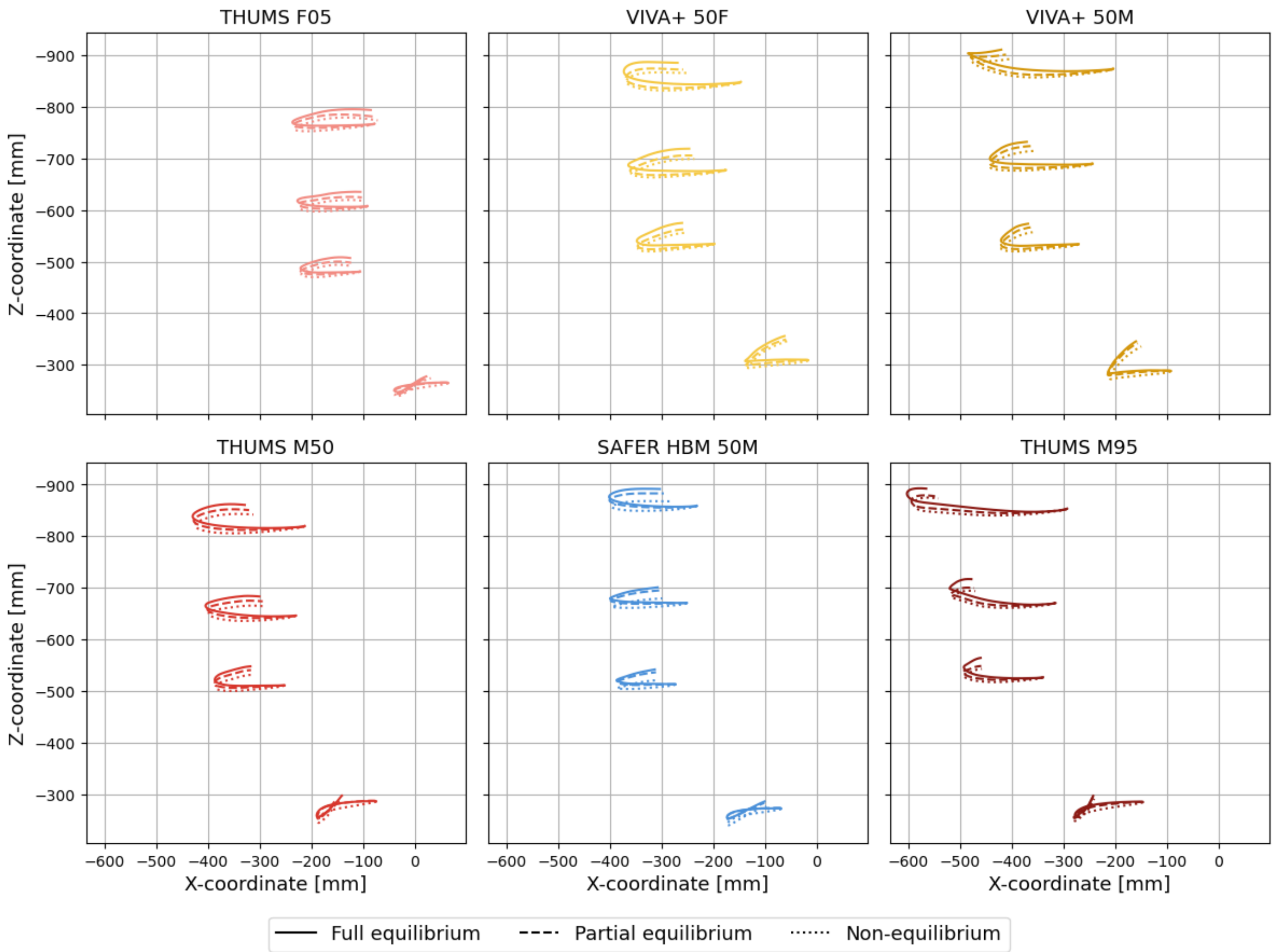

Fig. 3: Trajectories of the head, T1, T8 and pelvis in the rear end crash simulation, comparing the full equilibrium, to the partial and no equilibrium versions, for all six HBMs.

TABLE III
Differences in peak displacement in rear crash (mm)
Difference between PEq or NEq and FEq.
Font format: 0-10 mm (light gray), 10-15 mm (normal), **15+ mm (bold)**

		Head (x)	T1 (x)	T8 (x)	ASIS (x)	Head (z)	T1 (z)	T8 (z)	ASIS (z)
THUMS 05F	*PEq*	2.4	1.8	0.2	3.1	4.5	6.7	5.5	2.6
	NEq	3.2	3.6	1.7	5.0	11.8	13.2	11.6	9.7
VIVA+ 50F	*PEq*	3.8	3.6	1.8	4.6	13.2	10.1	10.0	7.2
	NEq	5.0	5.6	2.3	8.2	**19.7**	**15.6**	**15.5**	12.9
VIVA+ 50M	*PEq*	5.5	-0.1	0.3	0.2	7.1	8.6	8.0	3.1
	NEq	9.2	0.9	0.7	4.0	**17.0**	**15.6**	**15.3**	10.2
THUMS 50M	*PEq*	2.1	3.7	0.0	3.9	7.7	6.2	7.1	3.2
	NEq	5.1	6.1	1.2	4.8	**17.1**	**15.1**	14.9	12.2
	PEq	0.7	1.4	0.6	1.6	6.6	3.9	3.5	1.9

SAFER HBM 50M	*NEq*	5.3	3.8	1.3	3.2	**19.0**	**15.8**	**15.0**	14.3
THUMS 95M	*PEq*	8.6	2.0	-1.6	1.6	14.3	10.9	9.4	5.0
	NEq	13.5	2.7	-0.9	3.4	**20.3**	**17.1**	**15.8**	11.4

The contact forces for the rear crashes are shown in the Appendix as follows: Fig. A4, B4, C4, D4, E4, and F4 show contact force over time for all three equilibrium conditions between HBM and seat base (x- and z-direction), HBM and seat back (x- and z-direction), and HBM and rest (x- and z-direction); Figures A5, B5, C5, D5, E5, and F5 show peak contact force (independent of sign) for all three equilibrium conditions in all mentioned contacts. The differences in peak contact force for the rear crashes are summarised in Table IV. For most contacts and models, the PEq is closer to the FEq than the NEq. No clear pattern between the impact of using different methods and force direction was observed. Further, most contact forces differences, with the exception of the seat back contact in the x-direction (which represents the direction of loading, therefore resulting in a larger magnitude, see A4, B4, C4, D4, E4, and F4), stay under 250N.

TABLE IV
Differences in peak contact force in rear crash (N)
Difference between PEq or NEq and FEq.
Font format: 0-250 N (light gray), 250-500 N (normal), **500+ N (bold)**

		Seat base (x)	Seat back (x)	Head rest (x)	Seat base (z)	Seat back (z)	Head rest (z)
THUMS 05F	*PEq*	19	134	3	-31	-30	-7
	NEq	81	250	11	-64	-178	-4
VIVA+ 50F	*PEq*	-84	141	21	-116	-99	36
	NEq	-1	270	33	-141	-230	35
VIVA+ 50M	*PEq*	43	272	-16	-161	-39	65
	NEq	143	**505**	-31	-164	-117	65
THUMS 50M	*PEq*	103	72	-2	-99	-4	7
	NEq	151	308	6	-167	-91	32
SAFER HBM 50M	*PEq*	-131	64	-1	-25	-25	-24
	NEq	-156	337	-4	-51	-104	-29
THUMS 95M	*PEq*	102	248	-50	-53	-158	31
	NEq	209	268	-76	-165	-257	82

IV. DISCUSSION

This study evaluated the influence on HBM kinematics and kinetics during the crash phase, due to variations in initial equilibrium, attained by the system during the initialisation of a crash simulation. Two different crash scenarios, one frontal and one rear end, were investigated to generalise the results, as these represent different crash severities and different interactions with the vehicle interior. Additionally, six different HBMs, varying both in anthropometry and modelling techniques, were included to evaluate if there are systematic differences depending on body size and differences in modelling approaches. The results can be used to quantify the effect of (neglecting) equilibrium with the purpose of speeding up simulations, or to provide guidelines on how to apply damping, and for how long, to speed up the time to reach quasi equilibrium, in cases this is deemed important. When comparing the results of this study it should be done in the light of other sources of error, like numerical noise. In a previous study [18], it was shown that the variation in results between different numerical decompositions, for identical models, was in the same order as the differences seen between the three equilibrium conditions in the current study. Altogether, the results of the current study are useful for discussions around future virtual assessment methods.

It was found that the general recommendation to add global damping with a damping factor equal to 2ω (where ω is the highest eigenfrequency of the undampened system), when settling the HBM into the seat under gravity loading, resulted in an overdamped response. This response was expected, as both the seat foam and the HBM soft tissue includes damping on material level, and it can clearly be seen in Fig. A1, B1, C1, D1, E1, F1, comparing the magnitude of subsequent peaks, that the systems are quite damped already in the base line simulations. For the seat and the HBMs used in the current study the damping factor ranged from 0.196 to 0.276 ms^{-1}, and the time to reach quasi-static equilibrium ranged from 360 to 760 ms. No clear trends were found between HBMs representing different anthropometries or different modelling techniques. Here it should be mentioned that, as no stringent positioning method was used, it is possible that different HBMs were lifted a different amount (to clear from seat initial penetration), which in turn could contribute to the variability in time to equilibrium. These results can also be compared to the recommendations in [16] where the authors recommend 350 ms of settling time for upright occupants and 290ms for reclined, in both cases without global damping added. Given the large variability in settling times in the current study, it is unclear if the recommendations in [16] generalise to other seats and HBMs, something that the authors also listed as a limitation.

The kinematic and kinetic results are presented for all HBMs next to each other, see Fig. 2 and Fig. 3, and Table I through IV, and thus it is tempting to compare the results between HBMs. This comparison is not advisable for this study as this was not the objective the study was designed for. In other terms, as the aim was to compare the relative differences between different states of equilibrium *within* each HBM, no focus was put on making sure the different models (and anthropometrics) ended up in the most probable posture and position, for example using published regression models [24]. In particular, based on the trajectories in Fig. 2, it can be seen that the small female model submarines in the frontal crash load cases. As the seat model is not validated for this type of loading, and the HBM might be positioned too low relative to the steering wheel and driver airbag, it is not clear if this represents what would be the outcome in a real crash. Comparing the results between the three average sized HBMs makes more sense. However, even for these nominally similarly sized HBMs there are initial shape and posture differences, resulting in slight variations in seat initial position and arm and leg angles. One clear difference in the kinematic trajectories, see Fig. 2, is that the head moves further down and rebounds in a trajectory further down in the VIVA+ 50M model compared to the SAFER HBM and the THUMS M50. Analysing this in more detail shows that the spine, and in particular the lumbar spine, deforms (and buckles) differently in the VIVA+ model, but it can also be seen that the initial position of the VIVA+ hands is lower compared to the other two models at the start of the crash.

The influence of equilibrium within the HBMs for the different initialisation approaches can be seen to influence the kinematics of the torso and head, particularly in the rear impact. In the FEq simulations, the spine compresses by up to 20 mm during the gravity settling and achieves internal equilibrium, including in the spine and surrounding soft tissues. In the PEq simulation, however, equilibrium is reached locally only around the hip and thighs before the start of the crash. However, as the stresses in the discs in the spine were not initialised in PEq, these have to compress to form a new equilibrium, all the way up to the head, which results in the head moving an additional 10-20 mm downwards in the crash phase. In the NEq simulations no stresses were initialised and equilibrium needs to be formed all the way down from the seat foam up to the head. In practice, the difference was not so large compared to the PEq simulations, meaning the only recovering equilibrium locally around the hip and thighs is insufficient. Moreover, as the final HBM geometry from the gravity settling phase of FEq (with an already compressed spine) was used as the initial geometry of the PEq and NEq simulations, further reduction of the spine height results in further shortening of the spine in PEq and NEq compared to FEq. It should be noted that this results in a torso height that is even further away from the target anthropometry of the HBMs, as HBMs are modelled to match this target anthropometry (in their baseline, undeformed shape). Regardless of the initialisation approach, the HBMs can be expected to shorten (up to 20 mm) due to gravity loading over the course of a crash simulation because of the lack of internal stress initiation in the vertebrae discs. This is also observed through the kinetic behaviour. In particular, looking at the seat base z-force in both crashes and seat back z-force in the rear end crash, we consistently (with one exception) observe the seat exerting more force on the HBM in the PEq case and most in the NEq case, supporting the idea that the HBM spine and tissues compress and sink down into the seat after time zero. One trivial “fix” is to run the simulation without gravitational load, and this could possibly be motivated by crash accelerations being 10-40 times larger than the gravitational acceleration. Potentially this could work fine at least up to peak loading, and before the rebound phase, which in many cases is the important time frame for injury prediction anyway. The implications of the HBM height changing during a crash simulation, what it means to define a target anthropometry (in HBM development) or posture (for HBM positioning), needs further deliberation by the community. A more viable approach could be to include the possibility to initialise disc stresses to counterbalance the shortening due to gravity. However, the disc internal stress distribution will be dependent on posture (including recline angle), so it is not trivial to precompute a stress distribution that fits all purposes.

Two different crash configurations, in two directions, and with different crash severities, were used in this study. The frontal crash was a 70km/h, 37g, high severity crash, representative of NCAP crash pulses. In addition, 100 mm of instrument panel and steering wheel, and 200 mm of footwell intrusion were added. In this load case, the HBM interacts mainly with the driver's airbag, the seat belt, and the seat. As the initial posture of the HBMs were kept, the hands and arms were at different heights, and this meant that they interacted with the airbag differently. This is partly why the kinematics vary between HBMs, even if they were nominally of the same height. Additionally, the intruding instrument panel and steering wheel resulted in the airbag rotating inboards, twisting the HBM heads inboards. All this together makes HBM kinematics in this load case somewhat unpredictable, which can also be seen in Table I, where trends shift between HBMs. This can also be seen when looking at the kinetics. While some of the observed kinetic behaviour is to be expected, e.g. we see larger absolute differences for the seat base contact in the z- than in the x-direction, leading to more similar relative differences, other contacts vary to a higher degree (see e.g. DAB and Belt contacts in Table II). On the other hand, the rear end crash, with a delta velocity of 16km/h and peak acceleration of 10g, representative of a low severity rear end crash, produced much clearer kinematic and kinetic trends. Altogether, despite the difference in crash severities, the head dropped up to 20 mm in both load cases, meaning it strikes the airbag (in the frontal load case) or the head rest (in the rear end crash) at a lower position, compared to in the FEq simulations. This could also be one reason for the larger differences seen in the seat back x-direction in the rear end crash. As the HBMs hit the seat back at a lower position in the PEq- and NEq cases, the kinematic response of the seat becomes stiffer, thus exerting a larger reaction force on the HBMs.

The limitations of this study were that only HBM kinematics and kinetics were analysed. In future studies, the effect this has on injury risk should also be studied. This will help to further understand the influence of the downward motion and the internal stress state of HBM on the injury predictions. In addition, this study included only one seat model in the simulations. The design of the seat and particularly the seat stiffness may influence the procedure and time to reach equilibrium. Finally, the "full" equilibrium, used as baseline in this study, was not a true (static) equilibrium. Reaching a static equilibrium in an explicit FE code is not feasible, as the code solves the dynamic equilibrium equation, in contrast to implicit FE codes where the static equilibrium can be solved. In this study the ASIS velocity of 0.005 m/s, chosen to represent equilibrium, was rather arbitrary. However, at the time when the ASIS reached this velocity, the amplitude of the HBM oscillation was in the order of less than 1 mm, so it is not believed the results, and the conclusion of this study would change if the models had time to reach an even stricter equilibrium.

V. CONCLUSION

The approach used to initialise the equilibrium of an HBM influences the kinematics and kinetics during a crash, more in the vertical direction than in longitudinal direction. Given that HBMs lack internal stress initialisation, particularly in the spine, all HBMs can be expected to undergo a shortening of up to 20 mm due to gravity loading. This is also evident in the kinetic behaviours, where the effect of this compression of the spine and soft tissues is reflected in higher forces from the seat in the vertical direction. In the longitudinal direction the difference in peak displacement between a simulation including initial equilibrium and one without, was generally below 10 mm, resulting from the HBM interacting differently with the vehicle interior due to spine shortening. One such difference in vehicle interior interaction could be seen in the seat back contact in the rear end crash, where impact lower down on the seat back in the cases with partial- and no equilibrium could lead to higher forces from the seat due to a stiffer kinematic response. This study highlights the importance of defining consistent initialisation procedures that ensure comparable evaluations in virtual testing. Overall, the goal of the study was to take first steps towards establishing systematic approaches to initialisation of HBMs for virtual assessment by quantifying the effect it has on HBM responses in the crash phase.

VI. ACKNOWLEDGEMENTS

The simulations were enabled by computational resources provided by the National Academic Infrastructure for Supercomputing in Sweden (NAISS), partially funded by the Swedish Research Council through grant agreement no. 2022-06725. An initial version of this study was done as part of a bachelor's thesis project at Chalmers University of Technology. The project team consisted of Thim Högberg, Balder Lohman Ranheim, Hanna Mirkhan, Isac Sjövall, and Ellen Åkermo.

VII. REFERENCES

[1] Euro NCAP (2022) *Euro NCAP Vision 2030: a Safer Future for Mobility*, No. Euro NCAP Publication, .

[2] Edwards, M. (2023) Virtual testing will help us chart a new course in neck injury prevention, https://www.iihs.org/news/detail/virtual-testing-will-help-us-chart-a-new-course-in-neck-injury-prevention. [accessed 19 February 2025].

[3] Klug, C., Feist, F., et al. (2017) Development of a Procedure to Compare Kinematics of Human Body Models for Pedestrian Simulations. *Proceedings of IRCOBI Conference*, 2017, Antwerp, Belgium.

[4] Klug, C., Feist, F., et al. (2019) Development Of A Certification Procedure For Numerical Pedestrian Models. *Proceedings of 26th International Technical Conference on the Enhanced Safety of Vehicles (ESV): Technology: Enabling a Safer Tomorrow*, 2019, .

[5] Euro NCAP (2025) *Qualification Procedure for Human Body Models - Crash Protection*, No. CP 550 v1.1, .

[6] Euro NCAP (2025) *Human Body Model Simulation for Frontal Impacts - Crash Protection*, No. CP 551 v1.1, Euro NCAP, .

[7] Ressi, F., Schneider, B., et al. (2025) Development of a Robust Human Body Model Qualification Methodology: Ensuring Biofidelity for Occupant Protection Assessments in Virtual Testing. *Proceedings of IRCOBI Conference*, 2025, Vilnius, Lithuania.

[8] Fahse, N., Millard, M., et al. (2023) Dynamic human body models in vehicle safety: An overview. *GAMM-Mitteilungen*, **46**(2): p.e202300007. doi: 10.1002/gamm.202300007.

[9] Klein, C., Gonzalez-Garcia, M., et al. (2021) A Method for Reproducible Landmark-based Positioning of Multibody and Finite Element Human Models. *Proceedings of IRCOBI Conference*, 2021, .

[10] Beillas, P., Lafon, Y., et al. *D3.8 Final version of the personalization and positioning software tool with documentation. PIPER EU Project*, No. hal-01726335, IFSTTAR - Institut Français des Sciences et Technologies des Transports, de l'Aménagement et des Réseaux., .

[11] Ressi, F., Kofler, D., et al. (2020) Key Injury Regions for Passenger Car Drivers in Frontal Crashes: A Comparison of Results from IGLAD and Finite Element Simulations using a Human Body Model. *Proceedings of IRCOBI Conference*, 2020, Online.

[12] Poulard, D., Subit, D., et al. (2015) The Contribution of Pre-impact Posture on Restrained Occupant Finite Element Model Response in Frontal Impact. *Traffic Injury Prevention*, **16**(Sup2): pp.S87–S95. doi: 10.1080/15389588.2015.1064529.

[13] Leledakis, A., Östh, J., et al. (2022) The Influence of Occupant's Size, Shape and Seat Adjustment in Frontal and Side Impacts. *Proceedings of IRCOBI Conference*, 2022, .

[14] Putra, I. P. A., Iraeus, J., et al. (2022) Finite element human body models with active reflexive muscles suitable for sex based whiplash injury prediction. *Frontiers in Bioengineering and Biotechnology*, **10**p.968939. doi: 10.3389/fbioe.2022.968939.

[15] Iraeus, J., Mishra, E., Östh, J. (2023) Comparison of Average Female and Male Active HBM Responses in Whole-Sequence Frontal Crash Simulations. *Proceedings of IRCOBI Conference*, 2023, .

[16] Wade Von Kleeck, B., Caffrey, J., et al. (2024) Standardized Assessment of Gravity Settling Human Body Models for Virtual Testing. *Stapp Car Crash Journal*, **68**(1): pp.1–13. doi: 10.4271/2024-22-0001.

[17] LSTC (2020) *LS-DYNA® Keyword User's Manual, R12, Volume I*, Livermore Software Technology (LST), .

[18] Östh, J., Pipkorn, B., Forsberg, J., Iraeus, J. (2021) Numerical Reproducibility of Human Body Model Crash Simulations. *Proceedings of IRCOBI Conference*, 2021, Online.

[19] Safety Test Instrumentation Standards Committee (2022) *Instrumentation for Impact Test Part 1 - Electronic Instrumentation*, SAE International.

[20] SAE International Information Report (1994) *Sign Convention for Vehicle Crash Testing*, SAE International.

[21] Iraeus, J., Lindquist, M. (2016) Development and validation of a generic finite element vehicle buck model for the analysis of driver rib fractures in real life nearside oblique frontal crashes. *Accident Analysis & Prevention*, **95**pp.42–56. doi: 10.1016/j.aap.2016.06.020.

[22] VIRTUAL (2022) *Open Access Front Seat Model*, Https://openvt.eu/fem/open-access-front-seat-model.

[23] Euro NCAP (2025) *Crash Protection Rear Impact*, No. 1.1, Euro NCAP.

[24] Reed, M. P., Manary, M. A., Flannagan, C. A. C., Schneider, L. W. (2002) A Statistical Method for Predicting Automobile Driving Posture. *Human Factors: The Journal of the Human Factors and Ergonomics Society*, **44**(4): pp.557–568. doi: 10.1518/0018720024496917.

VIII. APPENDIX

A. Additional results for the THUMS 05F model

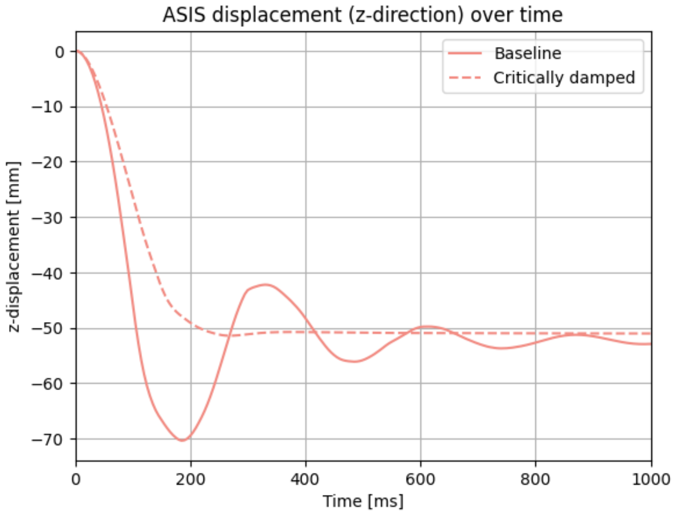

Fig. A1: The vertical displacement of ASIS node in the undamped transient (baseline) gravity loading and the near-critically damped gravity loading.

1) FRONTAL IMPACT

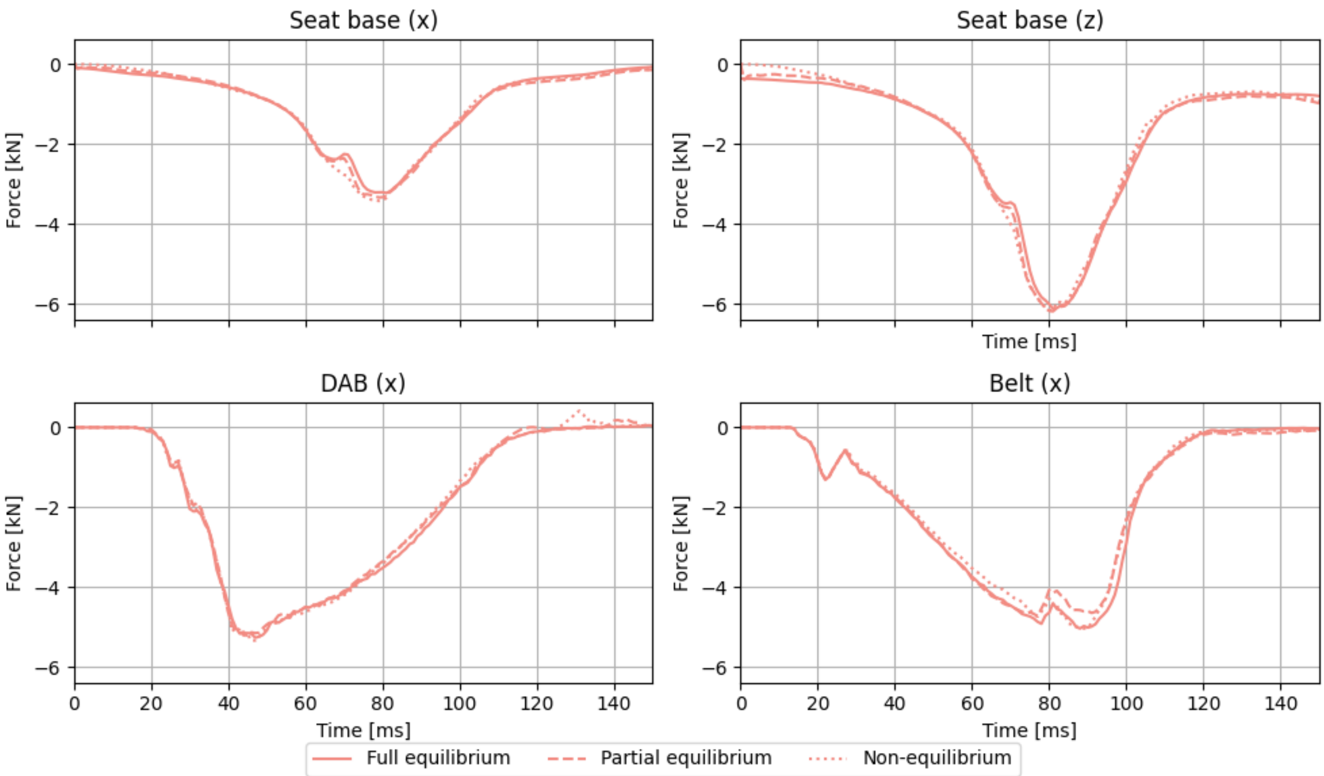

Figure A2: Contact forces in frontal impact

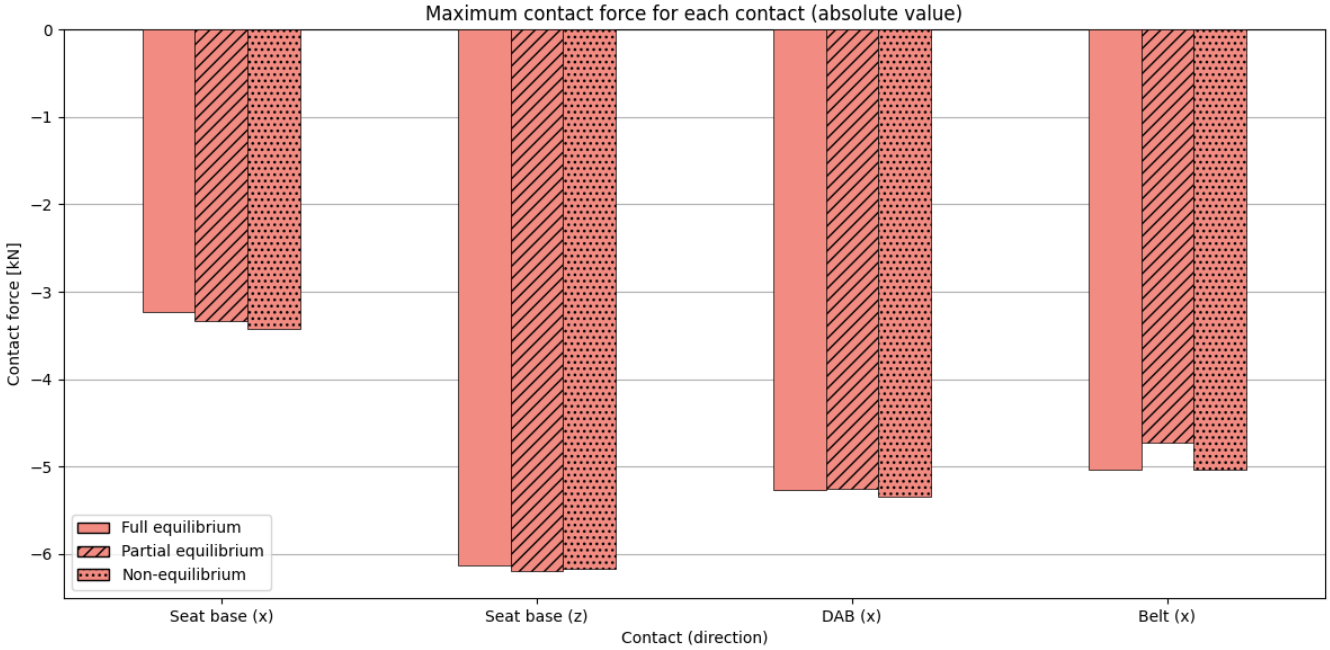

Figure A3: Maximum contact forces in frontal impact

2) Rear Impact

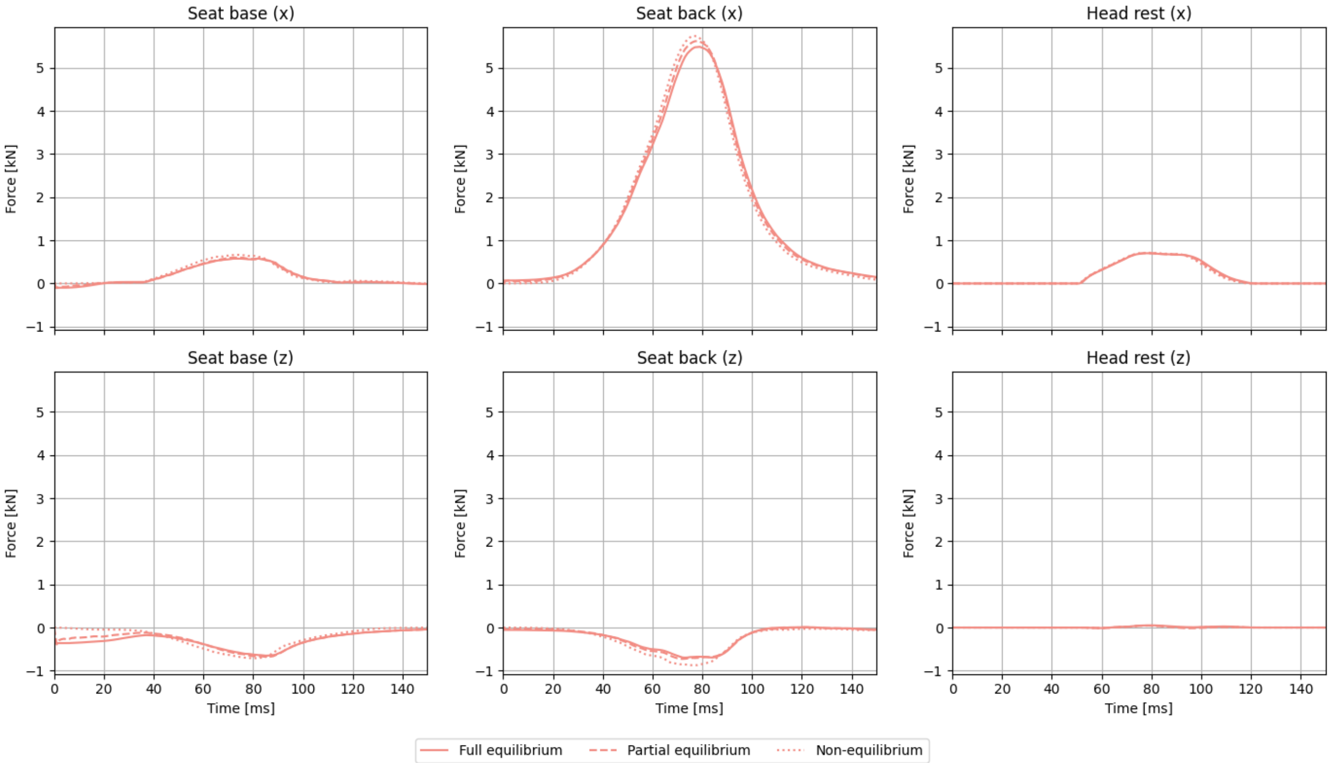

Figure A4: Contact forces in rear impact

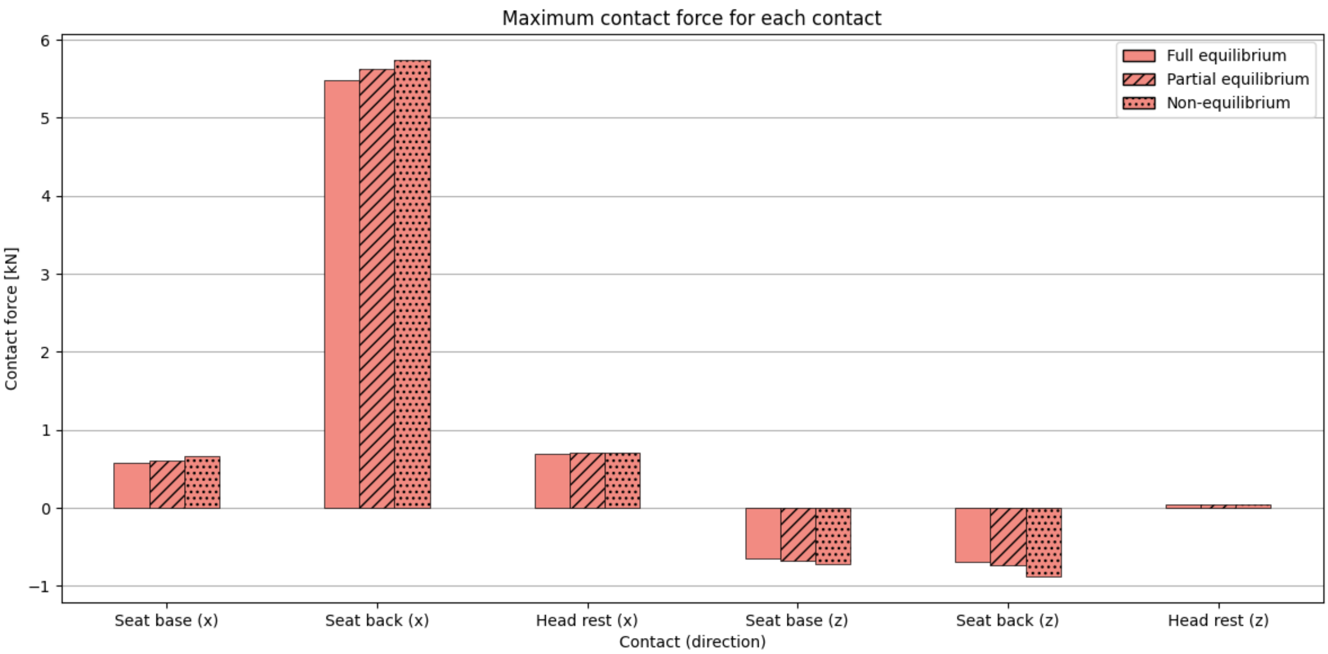

Figure A5: Maximum contact forces in rear impact

B. Additional results for the VIVA+ 50F model

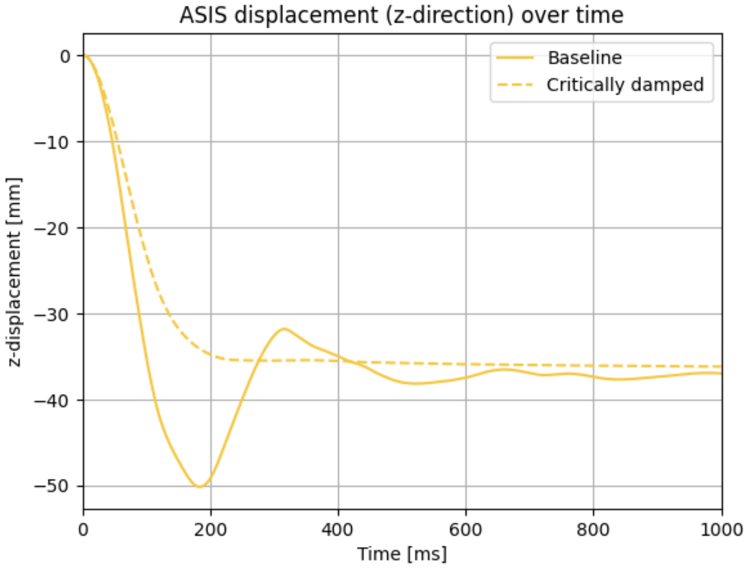

Fig. B1: The vertical displacement of ASIS node in the undamped transient (baseline) gravity loading and the near-critically damped gravity loading.

1) Frontal Impact

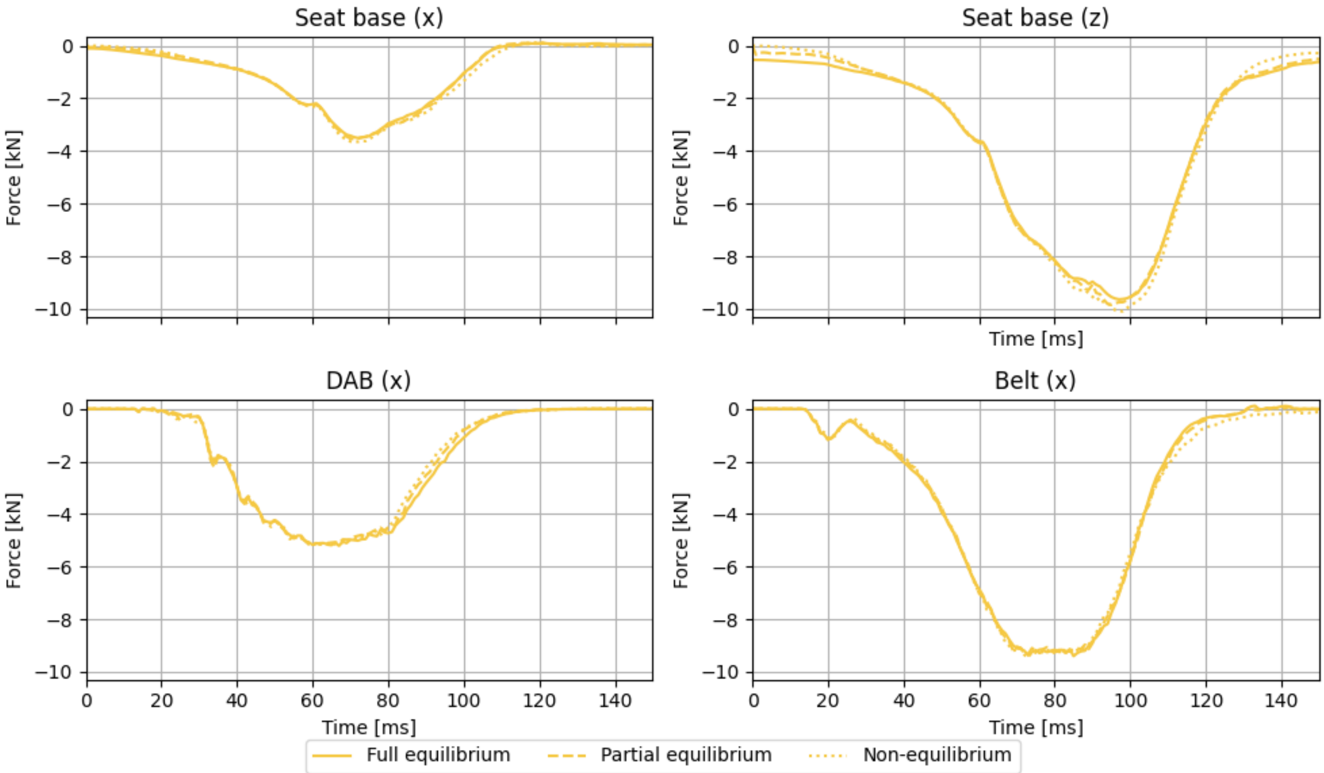

Figure B2: Contact forces in frontal impact

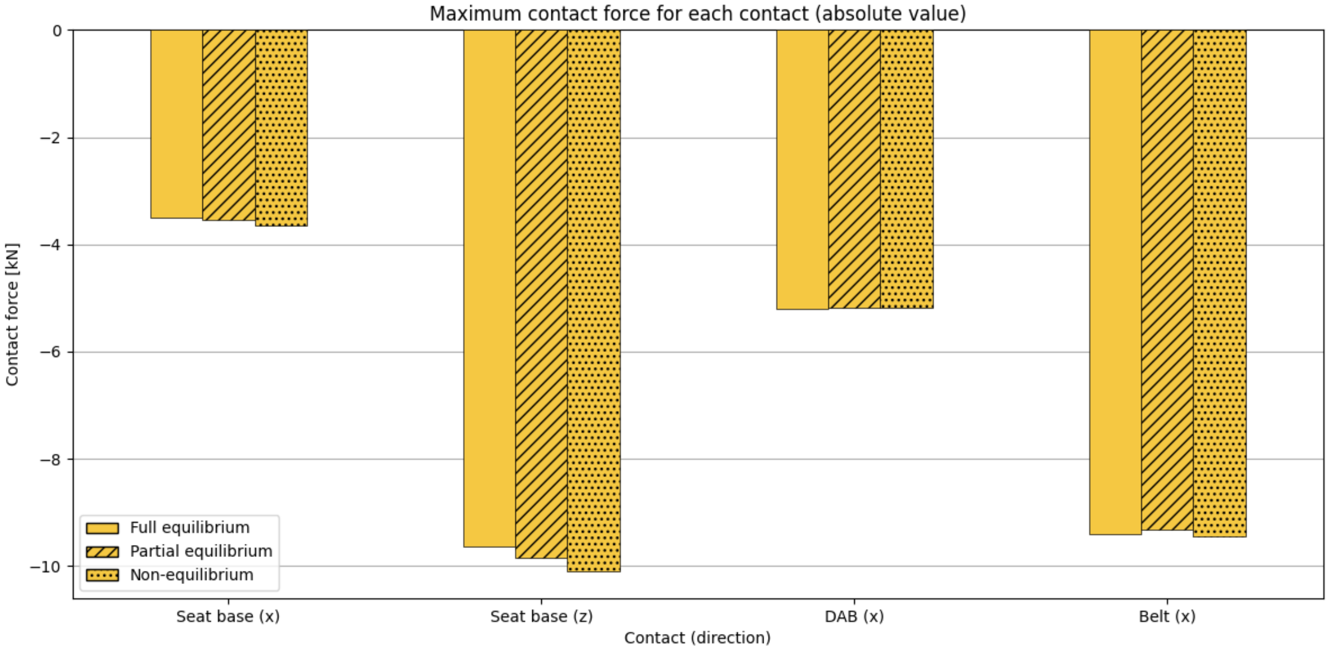

Figure B3: Maximum contact forces in frontal impact

2) Rear Impact

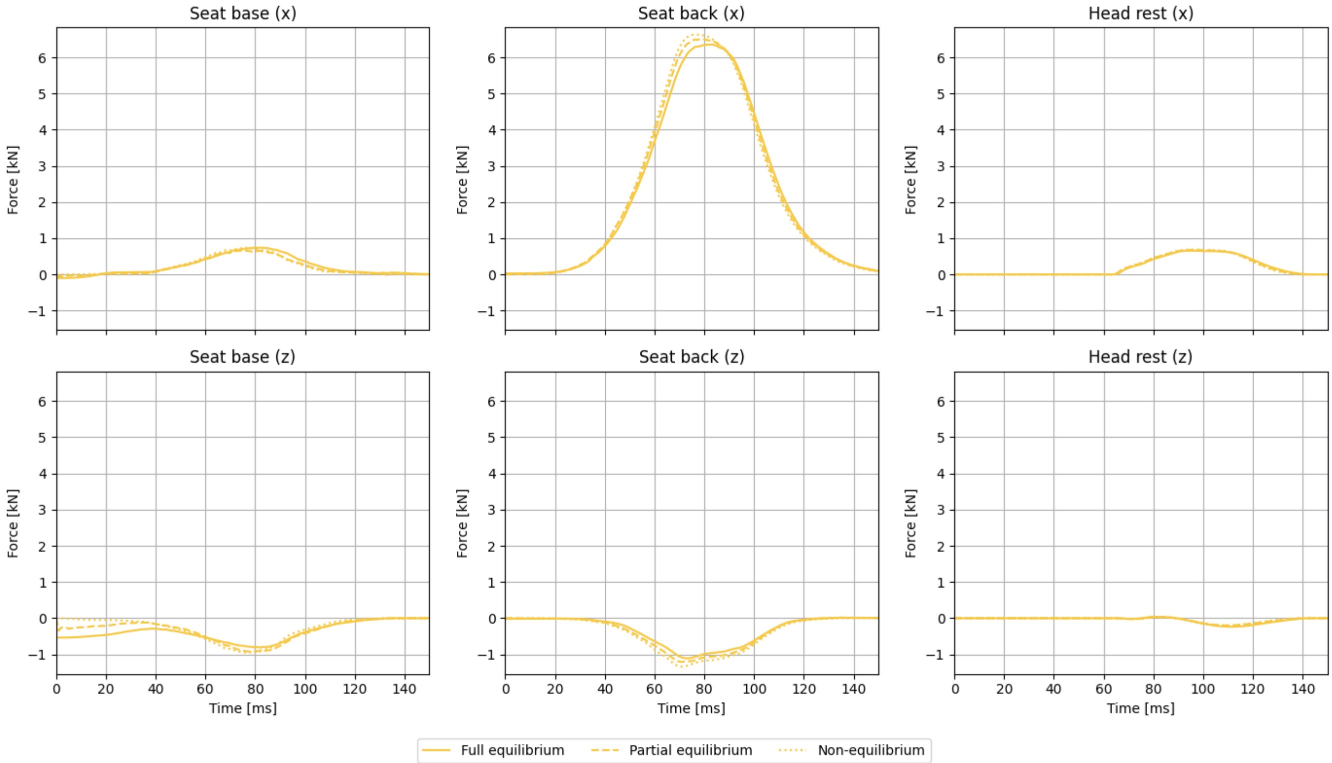

Figure B4: Contact forces in rear impact

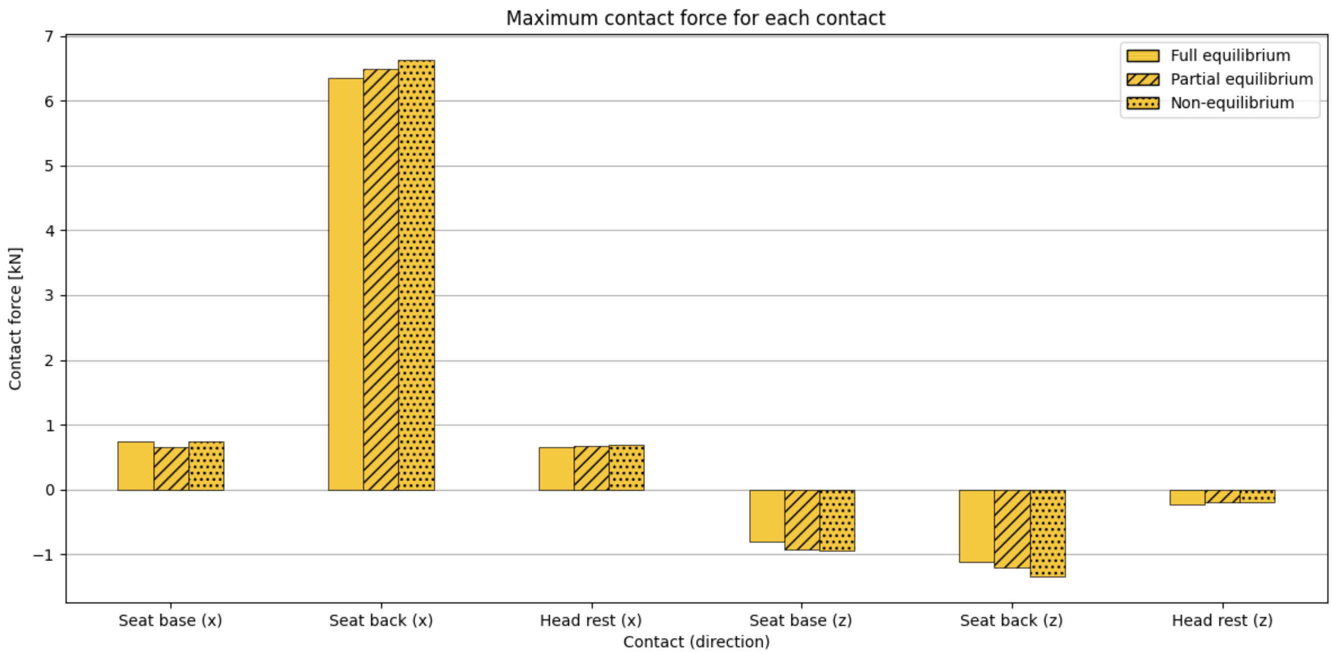

Figure B5: Maximum contact forces in rear impact

C. Additional results for the VIVA+ 50M model

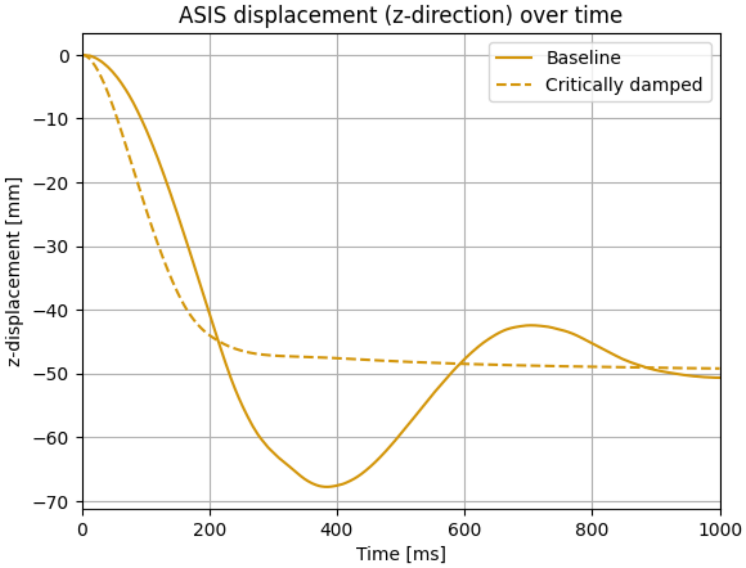

Fig. C1: The vertical displacement of ASIS node (VIVA+ 50F) in the undamped transient (baseline) gravity loading and the near-critically damped gravity loading.

1) FRONTAL IMPACT

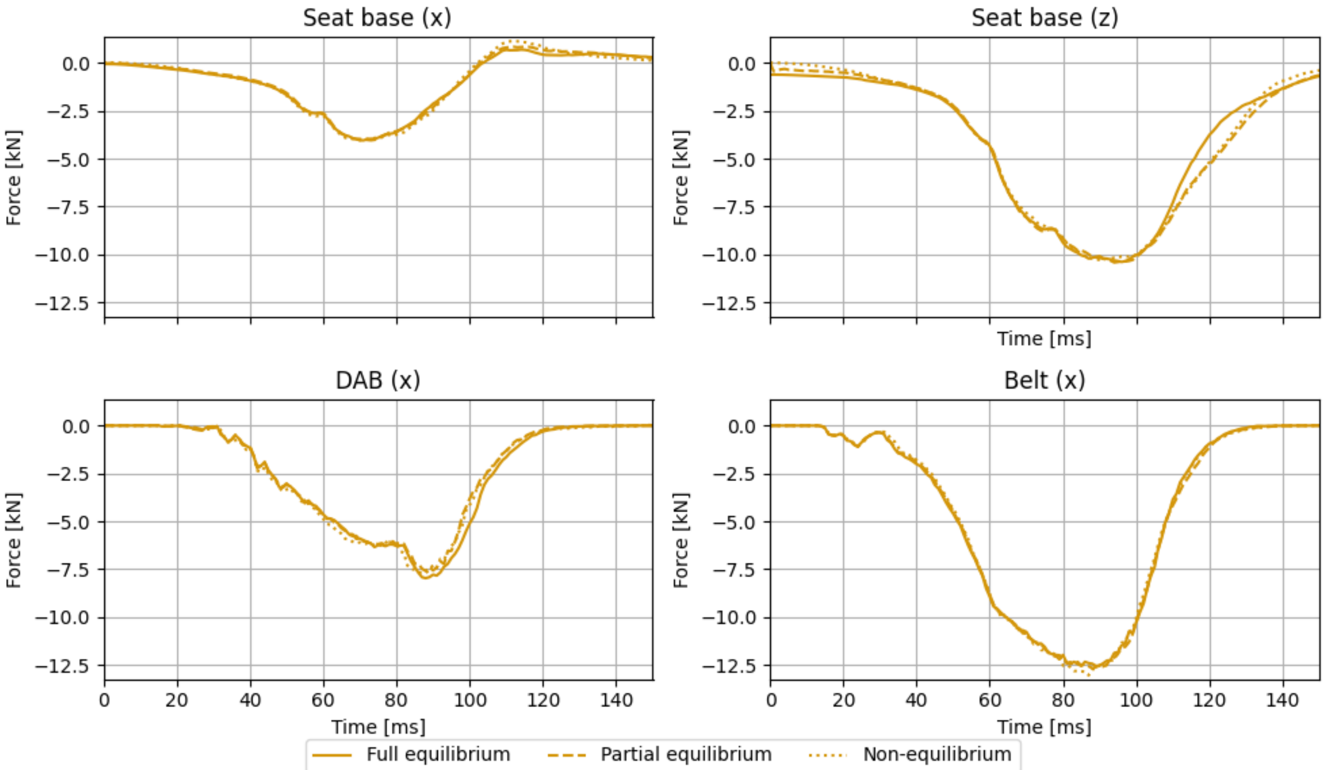

Figure C2: Contact forces in frontal impact

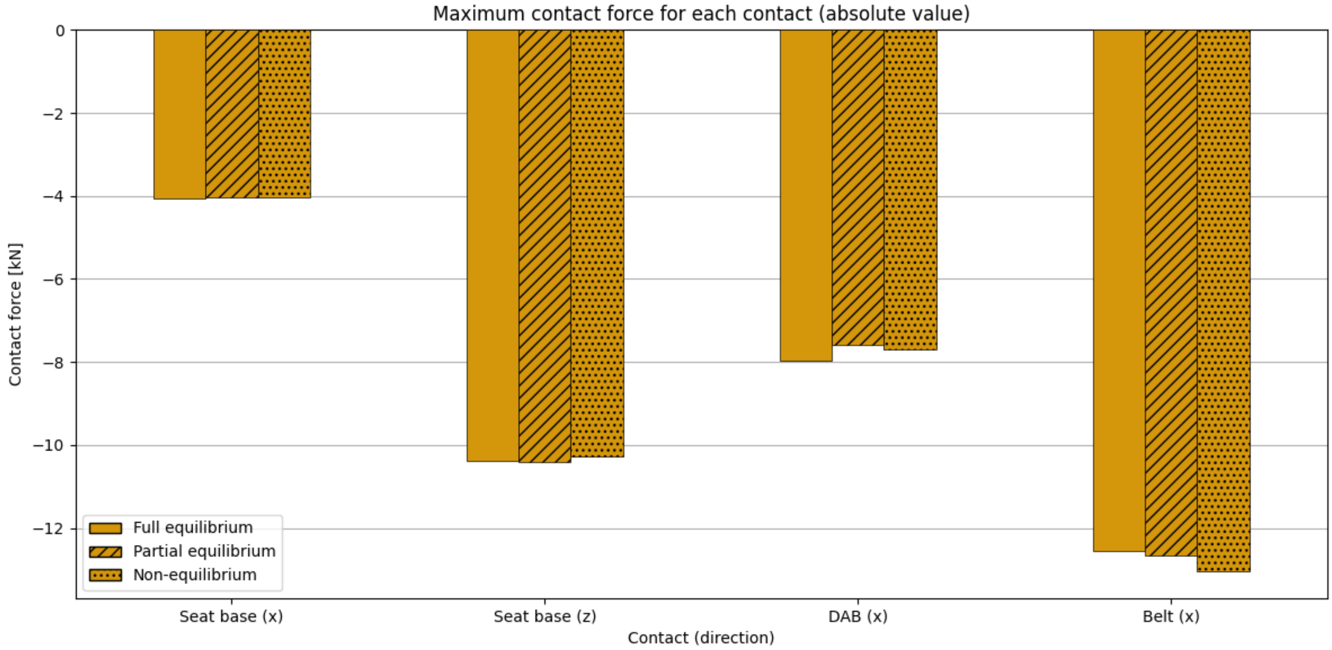

Figure C3: Maximum contact forces in frontal impact

2) Rear Impact

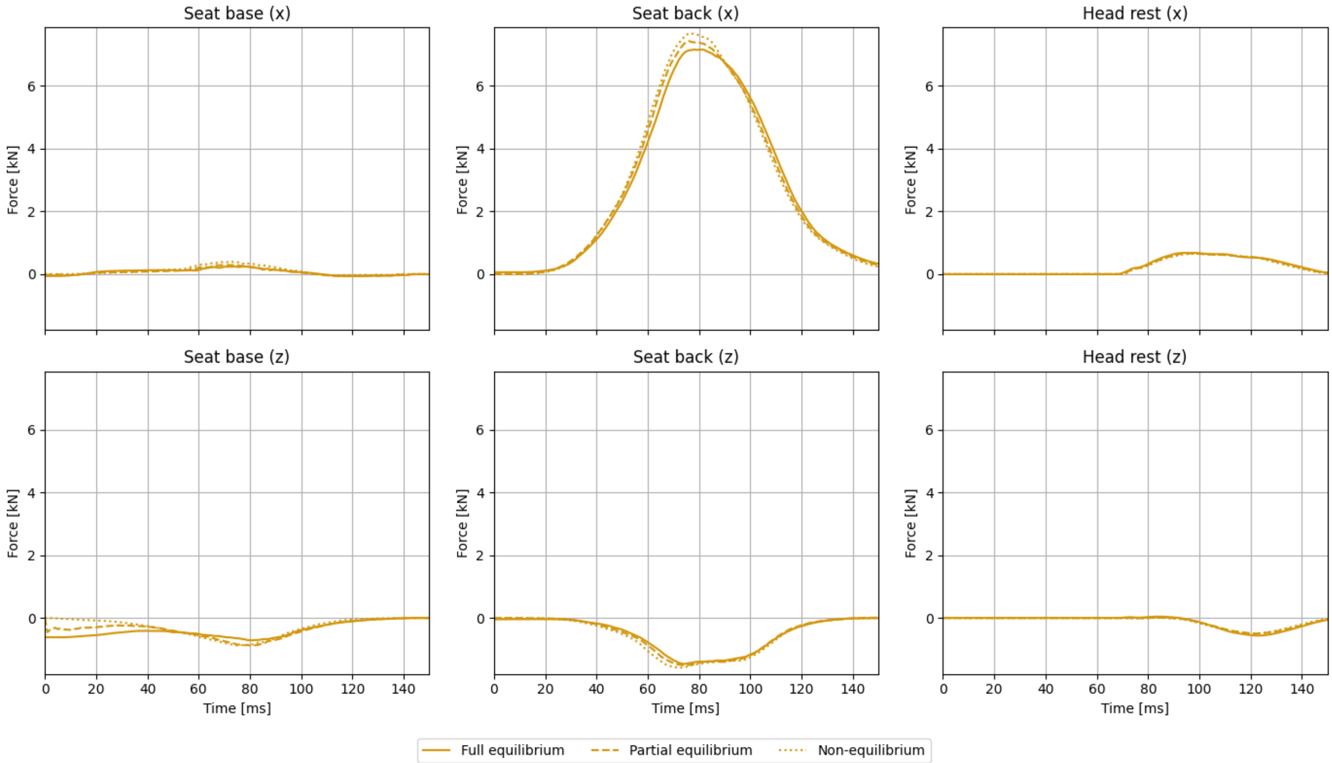

Figure C4: Contact forces in rear impact

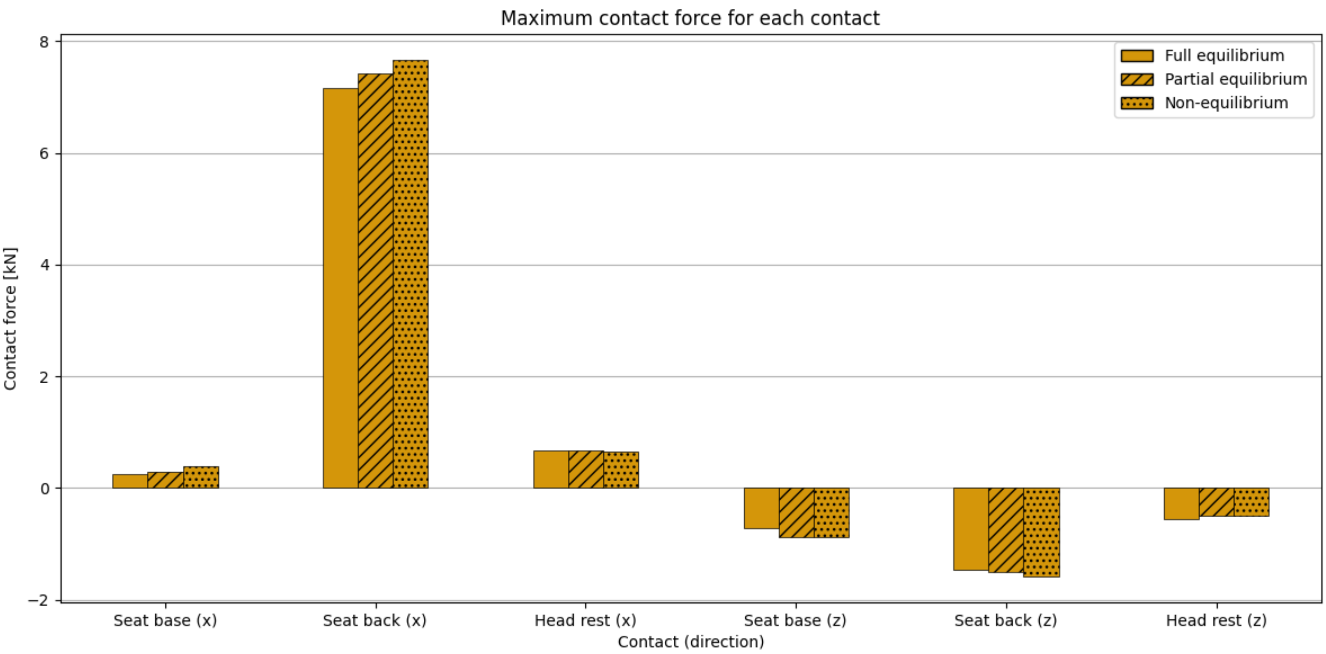

Figure C5: Maximum contact forces in rear impact

D. Additional results for the THUMS 50M model

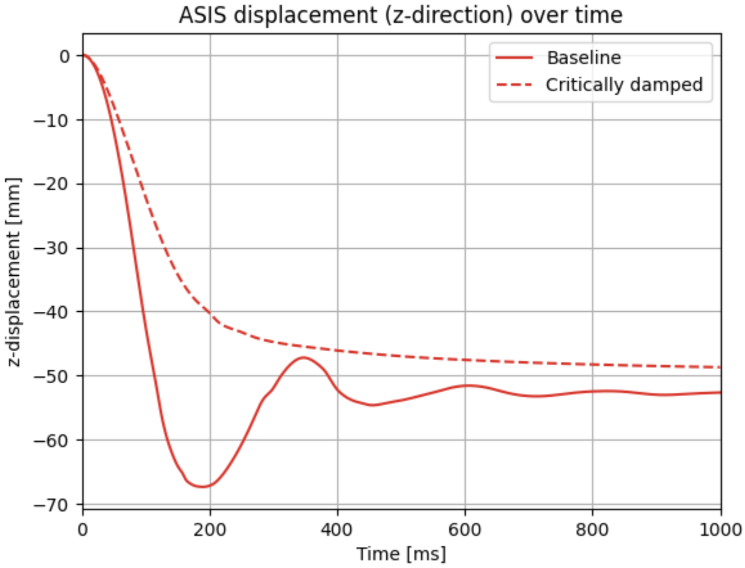

Fig. D1: The vertical displacement of ASIS node in the undamped transient (baseline) gravity loading and the near-critically damped gravity loading.

1) Frontal Impact

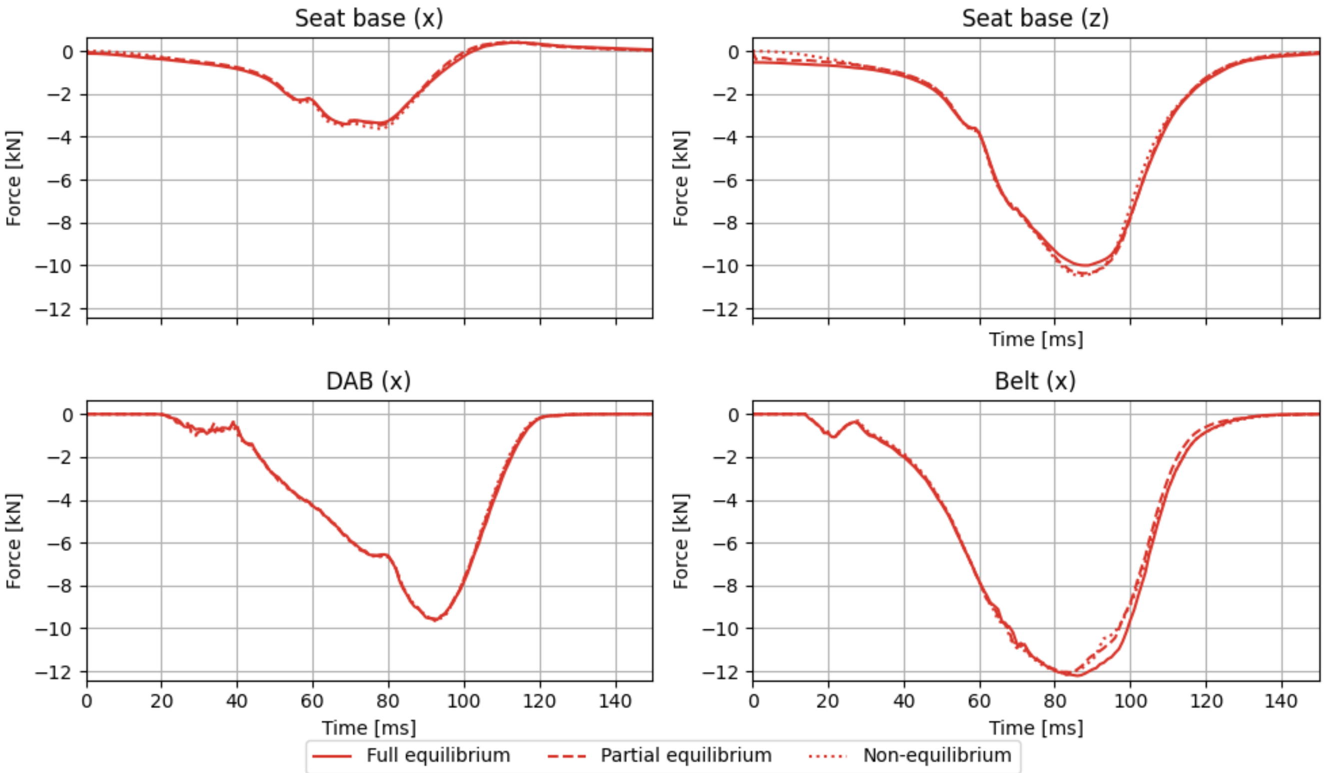

Figure D2: Contact forces in frontal impact

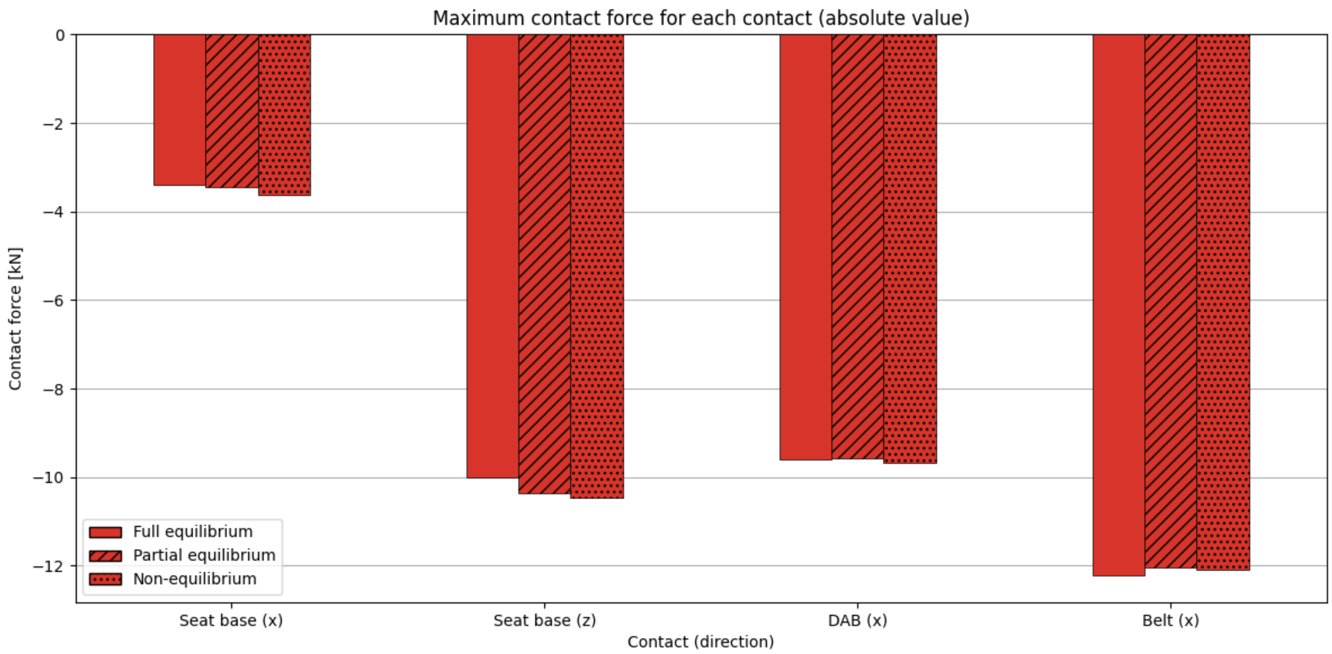

Figure D3: Maximum contact forces in frontal impact

2) Rear Impact

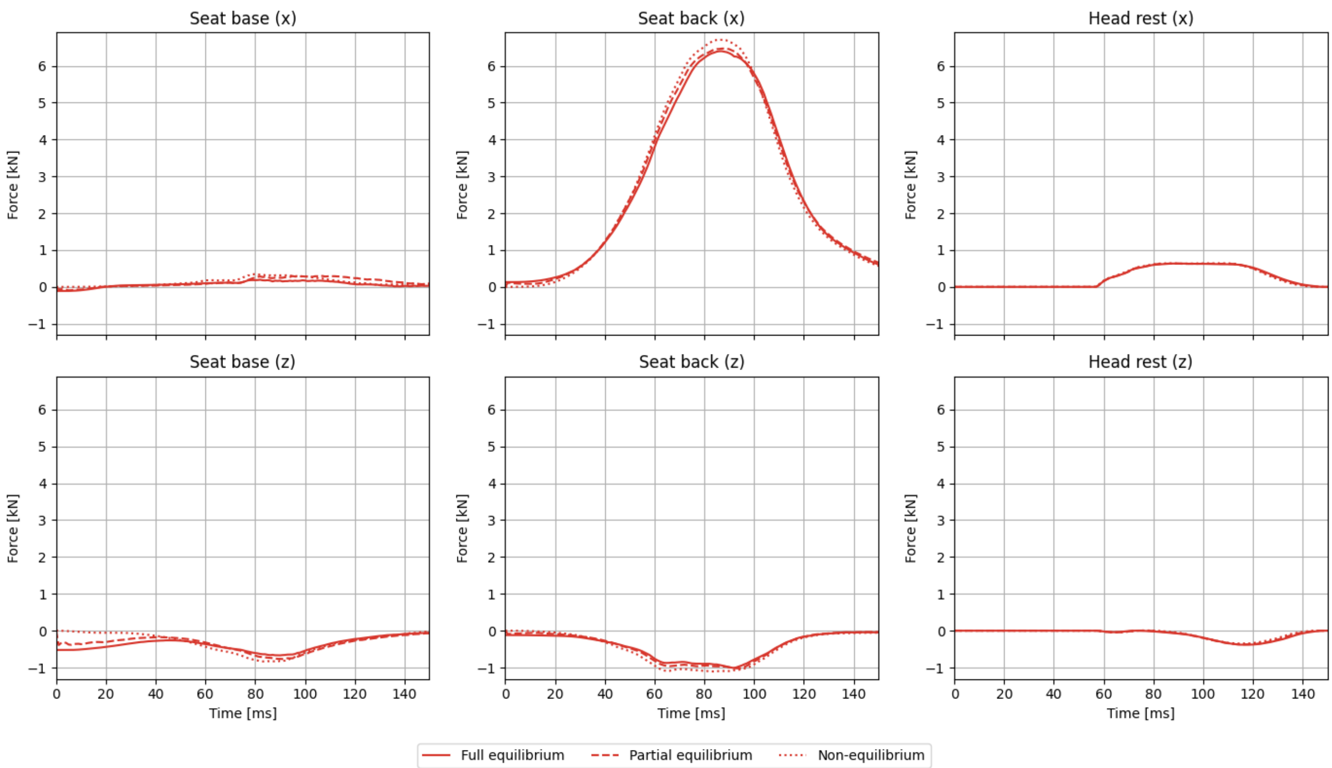

Figure D4: Contact forces in rear impact

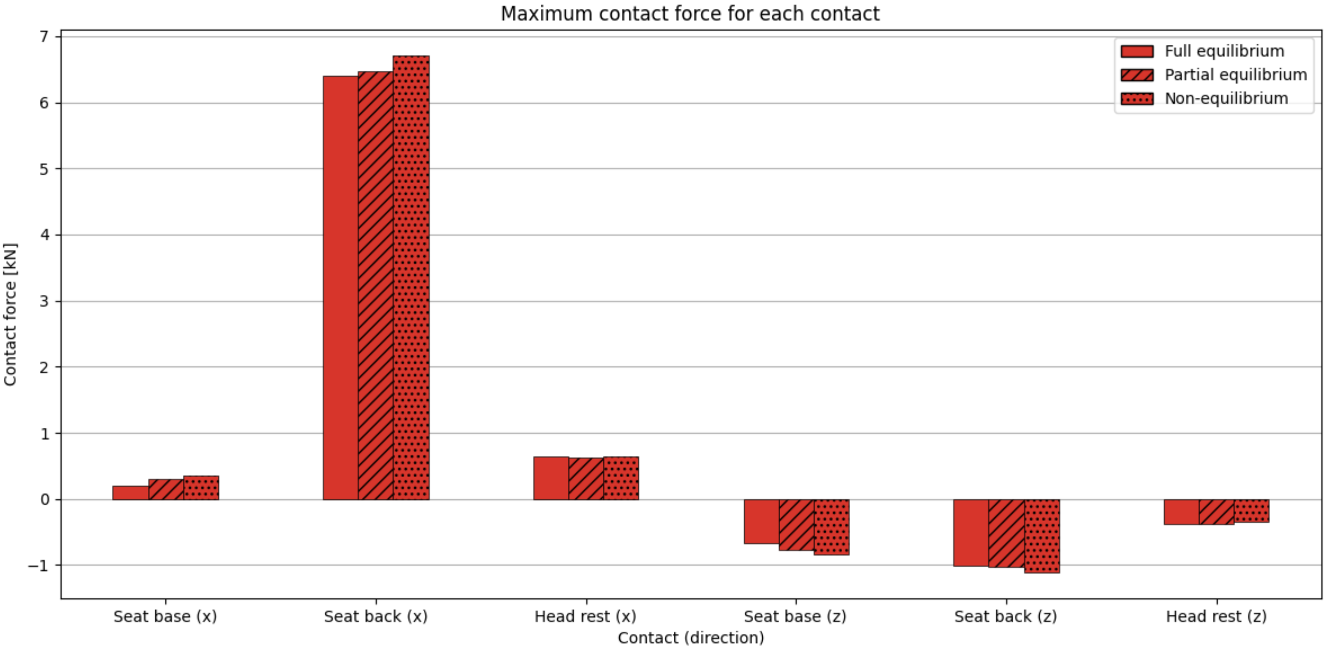

Figure D5: Maximum contact forces in rear impact

E. Additional results for the SAFER HBM 50M model

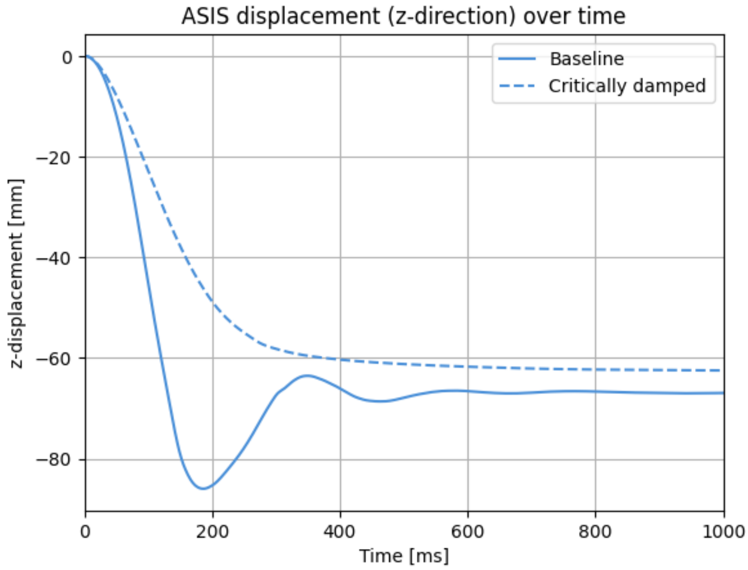

Fig. E1: The vertical displacement of ASIS node (VIVA+ 50F) in the undamped transient (baseline) gravity loading and the critically damped gravity loading.

1) Frontal Impact

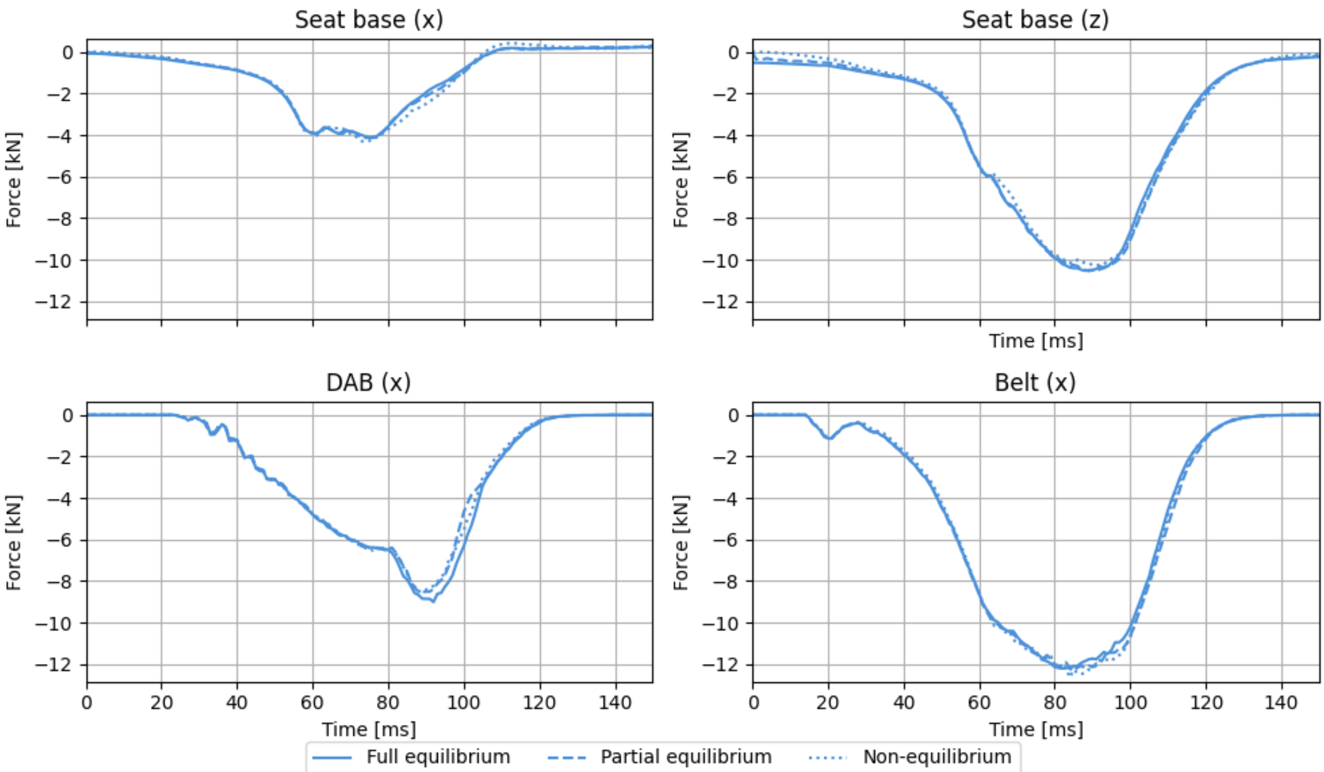

Figure E2: Contact forces in frontal impact

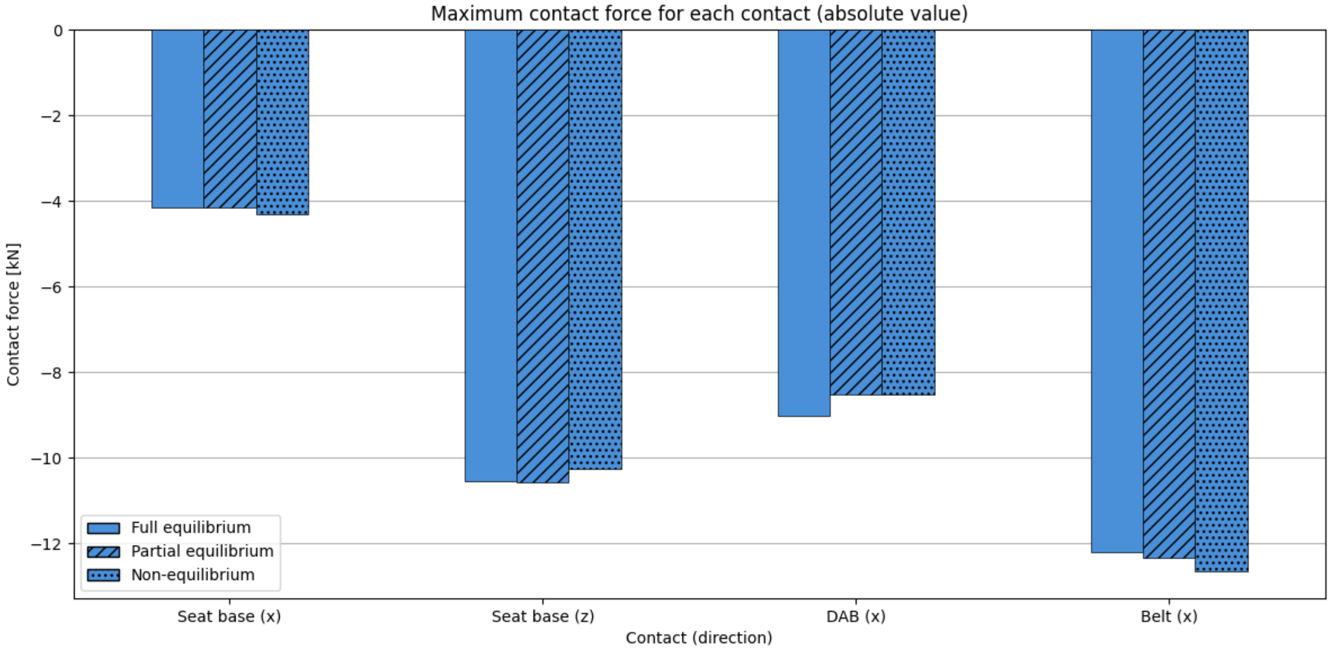

Figure E3: Maximum contact forces in frontal impact

2) Rear Impact

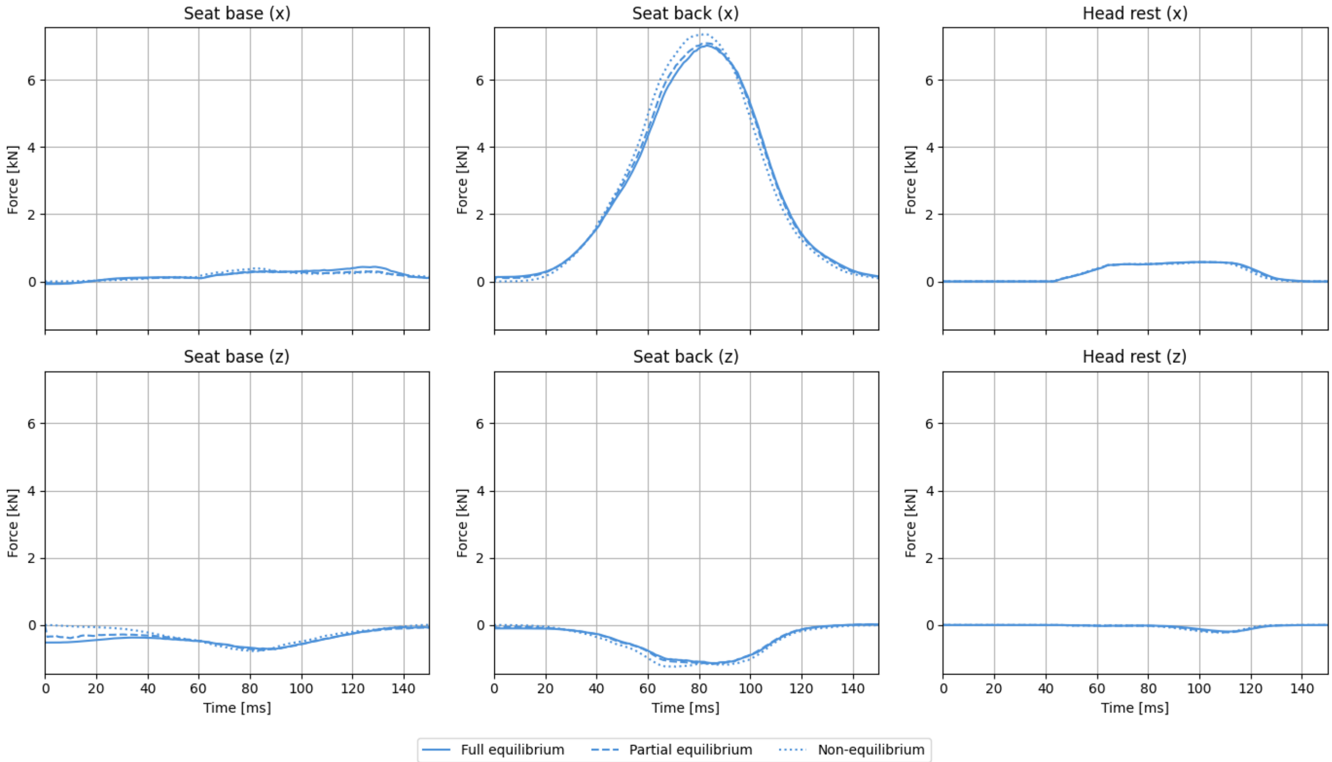

Figure E4: Contact forces in rear impact

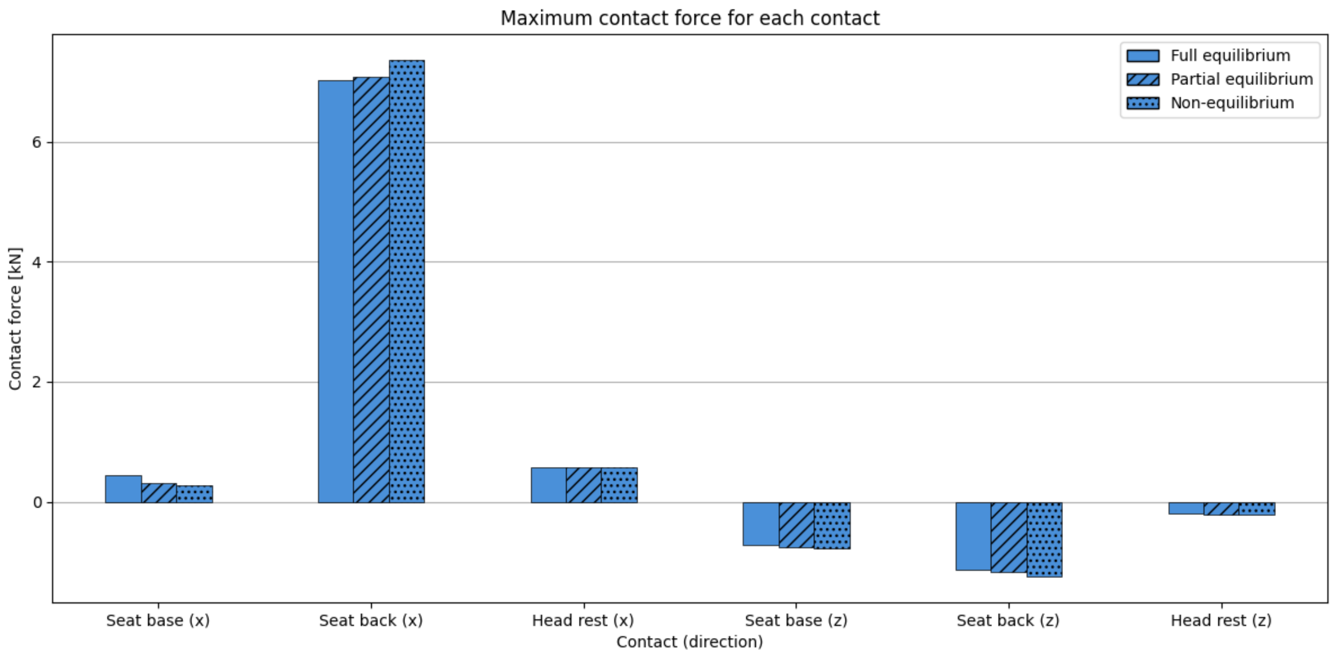

Figure E5: Maximum contact forces in rear impact

F. *Additional results for the THUMS 95M model*

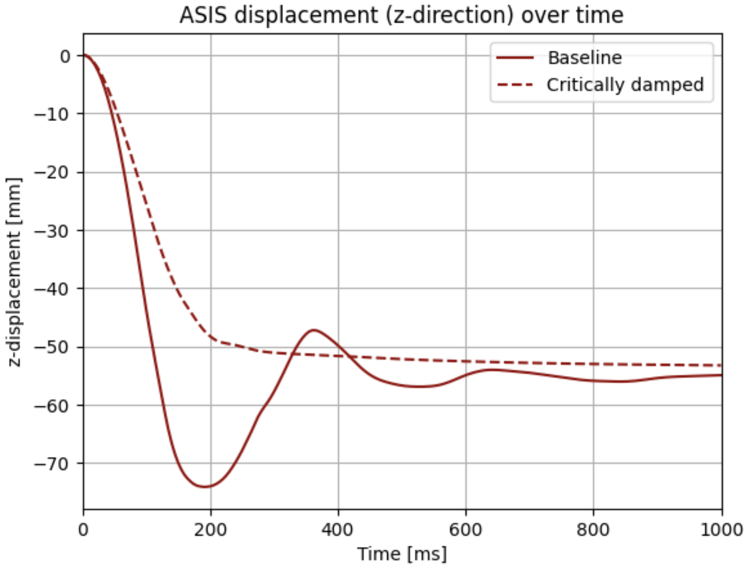

Fig. F1: The vertical displacement of ASIS node) in the undamped transient (baseline) gravity loading and the near-critically damped gravity loading.

1) *Frontal Impact*

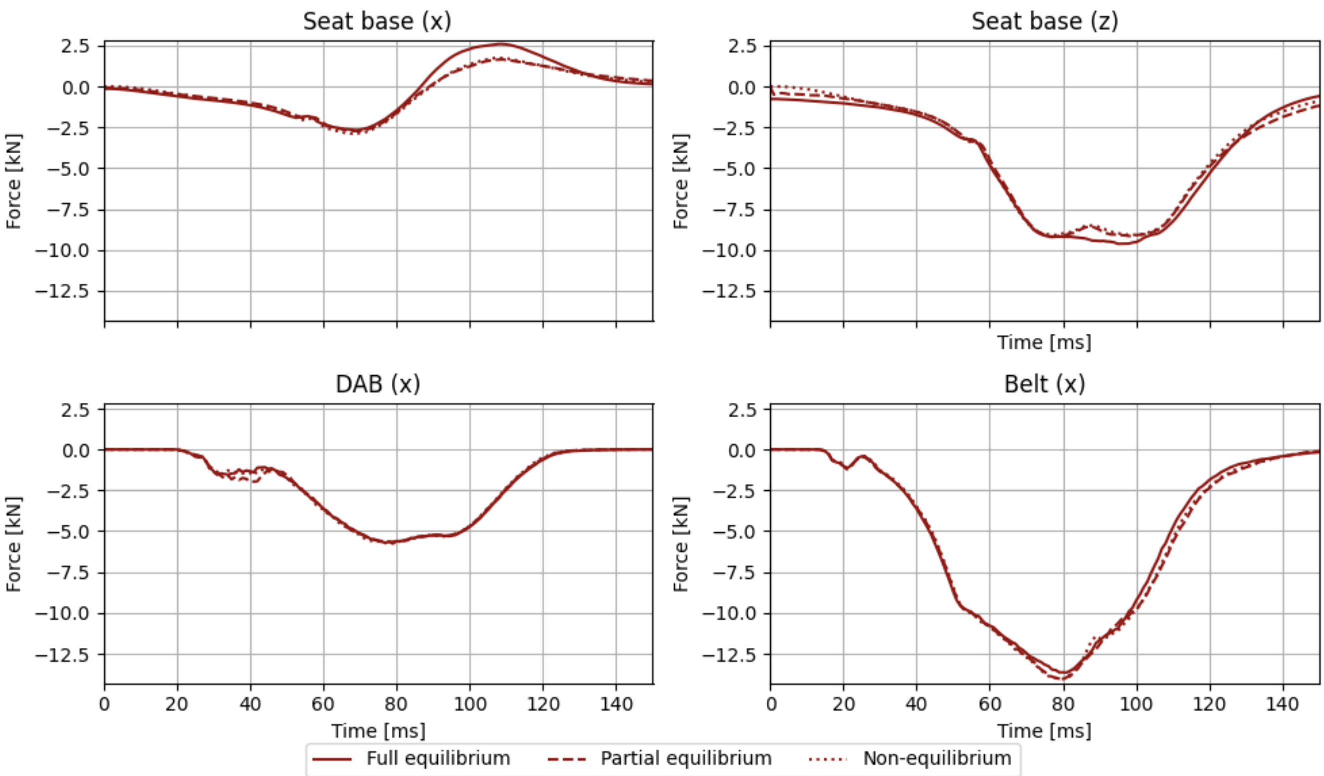

Figure F2: Contact forces in frontal impact

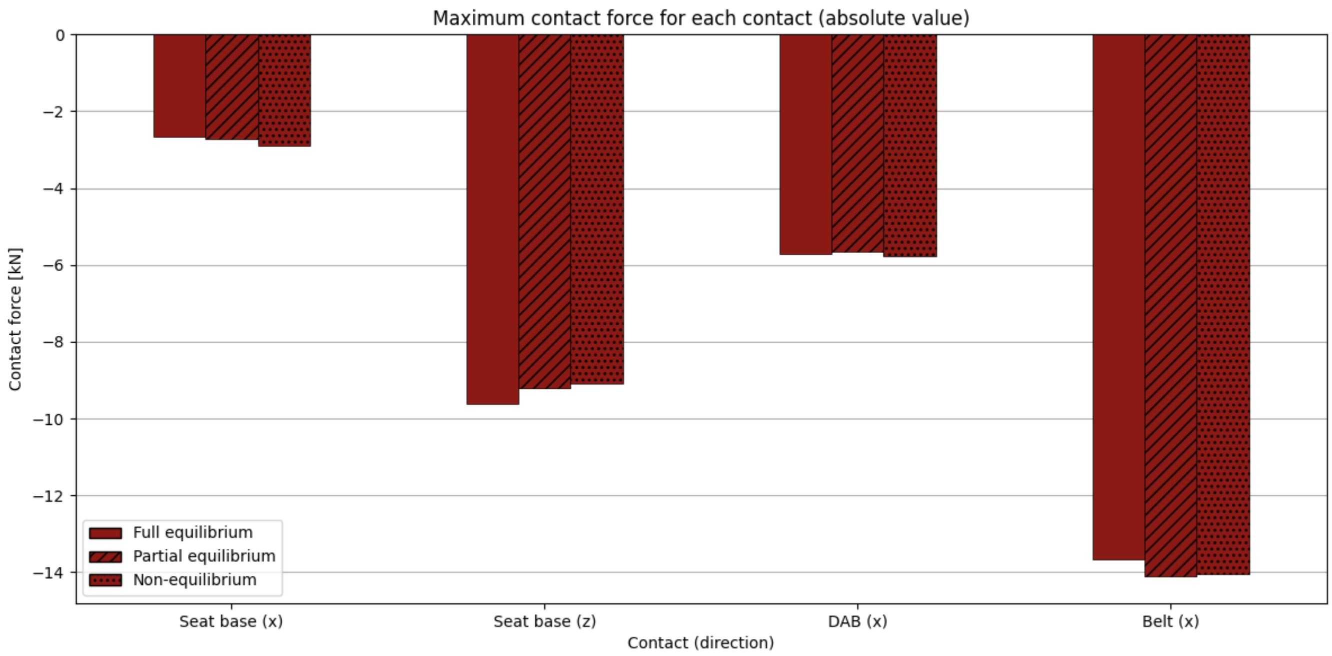

Figure F3: Maximum contact forces in frontal impact

2) Rear Impact

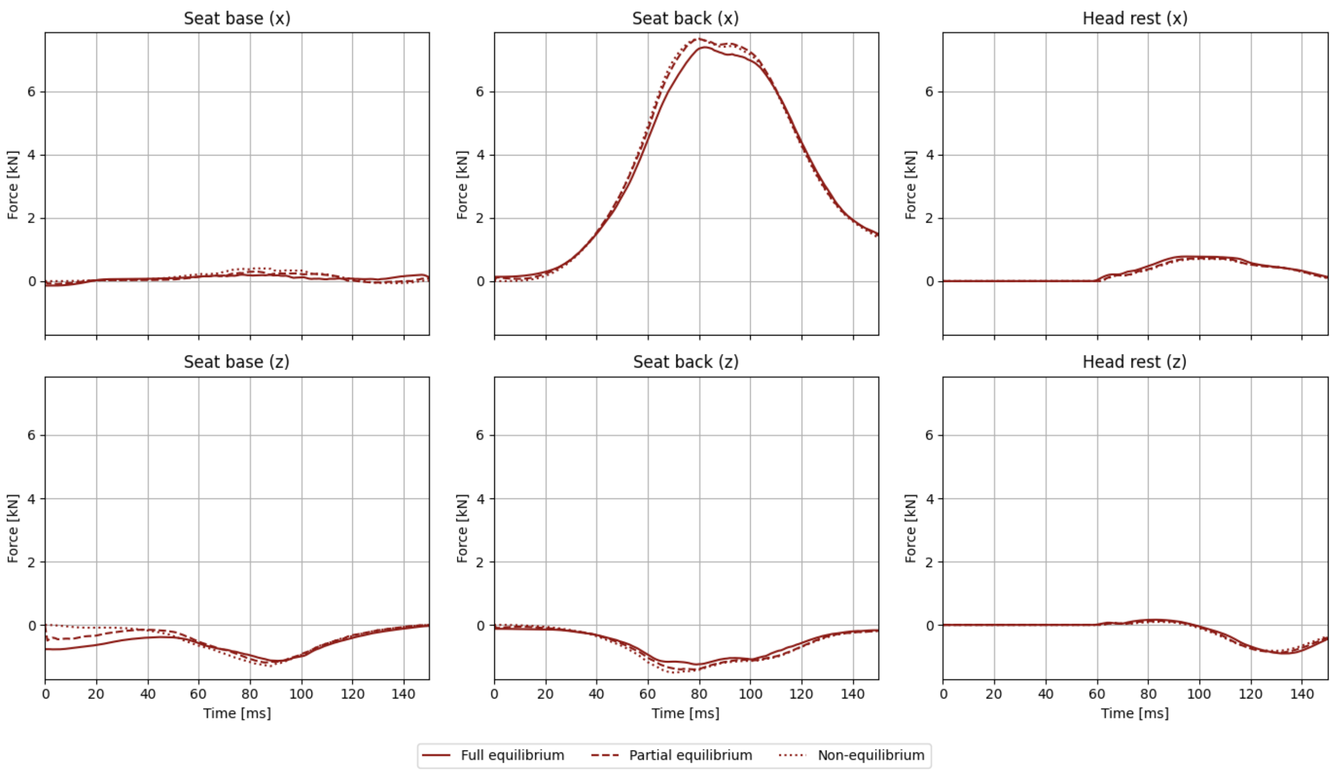

Figure F4: Contact forces in rear impact

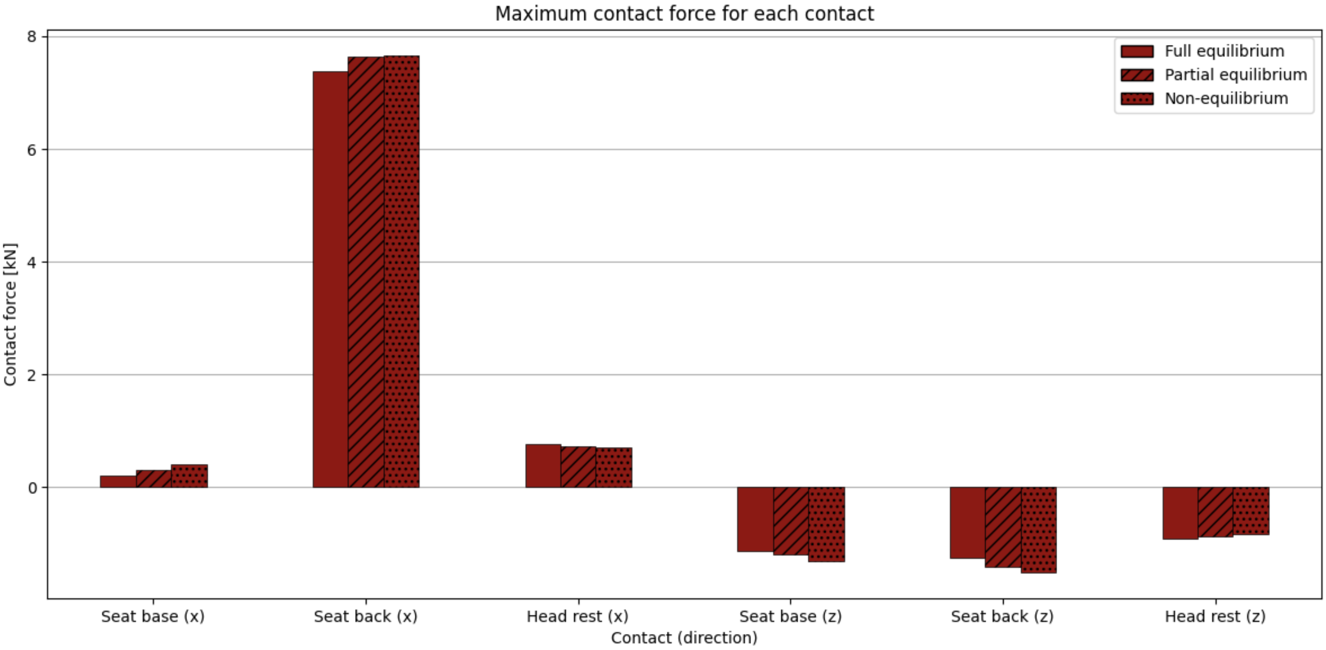

Figure F5: Maximum contact forces in rear impact